

Review

# Promising Methods for Corrosion Protection of Magnesium Alloys in the Case of Mg-Al, Mg-Mn-Ce and Mg-Zn-Zr: A Recent Progress Review

Pavel Predko <sup>1</sup>, Dragan Rajnovic <sup>2</sup>, Maria Luisa Grilli <sup>3</sup>, Bogdan O. Postolnyi <sup>4,5</sup>, Vjaceslavs Zemcenkovs <sup>1,6</sup>, Gints Rijkuris <sup>7</sup>, Eleonora Pole <sup>1,\*</sup> and Marks Lisnanskis <sup>1</sup>

- <sup>1</sup> SMW Group AS, Sintēzes iela 1, Mežgarciems, LV-2163 Carnikavas Novads, Latvia; pp@smw.com (P.P.); vjaceslavs.zemcenkovs@rtu.lv (V.Z.); ml@smw.com (M.L.)
- <sup>2</sup> Department of Production Engineering, Faculty of Technical Science, University of Novi Sad, Trg Dositeja Obradovica 6, 21000 Novi Sad, Serbia; draganr@uns.ac.rs
- <sup>3</sup> Casaccia Research Centre, Energy Technologies and Renewable Sources Department, ENEA—Italian National Agency for New Technologies, Energy and Sustainable Economic Development, Via Anguillarese 301, 00123 Rome, Italy; marialuisa.grilli@enea.it
- <sup>4</sup> IFIMUP—Institute of Physics for Advanced Materials, Nanotechnology and Photonics, Department of Physics and Astronomy, Faculty of Sciences, University of Porto, 687 Rua do Campo Alegre, 4169-007 Porto, Portugal; b.postolnyi@fc.up.pt
- <sup>5</sup> Department of Nanoelectronics and Surface Modification, Sumy State University, 2 Rymyskogo-Korsakova St., 40007 Sumy, Ukraine
- <sup>6</sup> Institute of Inorganic Chemistry, Faculty of Materials Science and Applied Chemistry, Riga Technical University, 3/7 Paula Valdena St., LV-1048 Riga, Latvia
- <sup>7</sup> Maritime Transport Department, Latvian Maritime Academy, 12 k-1, Flotes St., LV-1016 Riga, Latvia; gints@smw.com
- \* Correspondence: ep@smw.com



**Citation:** Predko, P.; Rajnovic, D.; Grilli, M.L.; Postolnyi, B.O.; Zemcenkovs, V.; Rijkuris, G.; Pole, E.; Lisnanskis, M. Promising Methods for Corrosion Protection of Magnesium Alloys in the Case of Mg-Al, Mg-Mn-Ce and Mg-Zn-Zr: A Recent Progress Review. *Metals* **2021**, *11*, 1133. <https://doi.org/10.3390/met11071133>

Academic Editor: Sebastian Feliú, Jr.

Received: 6 June 2021

Accepted: 10 July 2021

Published: 18 July 2021

**Publisher's Note:** MDPI stays neutral with regard to jurisdictional claims in published maps and institutional affiliations.

**Abstract:** High specific strength characteristics make magnesium alloys widely demanded in many industrial applications such as aviation, astronautics, military, automotive, bio-medicine, energy, etc. However, the high chemical reactivity of magnesium alloys significantly limits their applicability in aggressive environments. Therefore, the development of effective technologies for corrosion protection is an urgent task to ensure the use of magnesium-containing structures in various fields of application. The present paper is aimed to provide a short review of recent achievements in corrosion protection of magnesium alloys, both surface treatments and coatings, with particular focus on Mg-Al-Mn-Ce, Mg-Al-Zn-Mn and Mg-Zn-Zr alloys, because of their wide application in the transport industry. Recent progress was made during the last decade in the development of protective coatings (metals, ceramics, organic/polymer, both single layers and multilayer systems) fabricated by different deposition techniques such as anodization, physical vapour deposition, laser processes and plasma electrolytic oxidation.

**Keywords:** magnesium alloys; corrosion; corrosion protection; coatings



**Copyright:** © 2021 by the authors. Licensee MDPI, Basel, Switzerland. This article is an open access article distributed under the terms and conditions of the Creative Commons Attribution (CC BY) license (<https://creativecommons.org/licenses/by/4.0/>).

## 1. Introduction

Corrosion of metals is a determining factor that limits their usage, potential applications and operational conditions. Only a complete understanding of the corrosion processes under certain circumstances makes it possible to choose an appropriate protection method.

High specific strength characteristics make magnesium alloys widely demanded in many industrial applications such as aviation, astronautics, military, automotive, bio-medicine, energy, etc. However, the high chemical reactivity of magnesium alloys significantly limits their applicability in aggressive environments. Therefore, the development of effective technologies for corrosion protection is an urgent task to ensure the use of magnesium-containing structures in various fields of application. It should be noted that,

in a contrast to steels or aluminium alloys, magnesium-based alloys exhibit a much higher resistance to stress corrosion cracking (SCC) and they are highly resistant to intergranular and exfoliating corrosion at the same time (except in the case of magnesium-lithium alloys) [1,2].

The demand for highly durable lightweight materials in the production of wear and corrosion-resistant components for reliable applications in the construction of aircrafts, cars, trains, ships, and military defence equipment has become critically high for market capacity. Researchers working on almost every type of materials are looking for a better combination of properties, e.g., the highest payload/density ratio: polymers and composites [3–5], metal matrix composites (iron-based [6–9]; steel-based [10,11]; Mg-based [12–14]); metal-ceramics [15–18]; ceramics and composites [19–24]; bio-based and hybrid materials [15,25].

Such lightweight metals and alloys like Mg- and Al-based materials possess high strength-to-weight ratios and low density [26], as demonstrated in Table 1. Common applications are met in the automotive, aerospace, manufacturing, railway and other large niche fields. For example, lighter vehicles consume less fuel, emit less CO<sub>2</sub> and NO<sub>x</sub> and provide better performance. In the aviation sector, for instance, there is an increasing demand for new aircrafts able to satisfy the requirement of aviation programs ACARE 2020 (Advisory Council for Aviation Research and Innovation in the EU) and Flightpath 2050. A reduction of fuel consumption as well as CO<sub>2</sub> and NO<sub>x</sub> emissions in the next 30 years [27] are the main goals in the frameworks of these programmes. The aforementioned sectors are of crucial importance for the European Manufacturing Industry in accordance with recently published Eurostat data [28]. These sectors currently provide more than 6 million jobs and contribute ~11% to the EU-28's GDP (gross domestic product). The main end-use applications of magnesium in the EU are demonstrated in Figure 1.

**Table 1.** Strength, processing energy, emissions and density for aluminium and magnesium [29,30].

Properties	Al	Mg
Density (kg·m <sup>-3</sup> )	2700	1738
Strength-to-Weight Ratio (kN·m·kg <sup>-1</sup> )	130	158
Processing Energy (kW·h·kg <sup>-1</sup> )	56	43
Emissions (kg[CO <sub>2</sub> ]·kg <sup>-1</sup> )	22	6.9

Aluminium, magnesium, and titanium alloys are the most frequently applied lightweight metals in the industry [31]. Magnesium is an ecologically friendly material with less CO<sub>2</sub> emission and manufacturing footprints from manufacturing processes, as compared to aluminium [32]. Therefore, the production and processing of magnesium possess a much lower polluting impact on the environment. Magnesium also has superior characteristics as compared to other weight and stress-loaded elements or structural materials. It should be noted that magnesium is significantly (35%) lighter than aluminium [29,30], as demonstrated in Table 1. The lightweight metals Al and Mg have the potential to play a significant role in future energy-saving efforts across a wide range of applications, including transport, power generation, industrial processing, construction and many other fields. The high strength-to-weight ratios of these metals would lead to the production of more fuel-efficient vehicles without the impact on performance or safety. Titanium has greater natural corrosion resistance, while Al is often alloyed with Mg to provide higher ductility, weldability, and corrosion resistance [29,30].

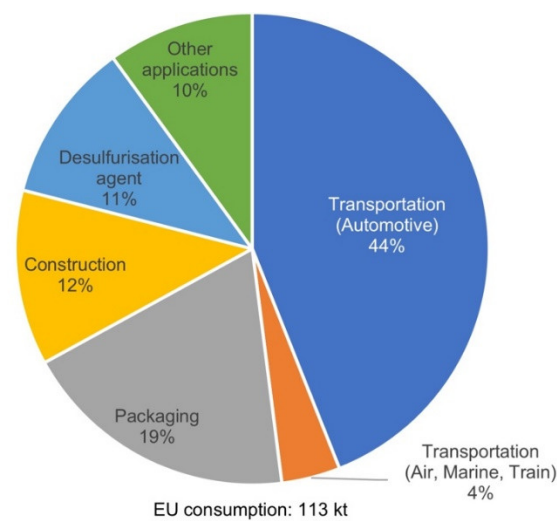


**Figure 1.** End-use of magnesium in the EU, in period 2012–2016. Adapted from [33].

The 1970's oil crisis caused the demand for reduced weight in transport systems. Many efforts have successfully resulted in improved energy efficiency [34]. Especially, the addition or complete replacement of heavy metals with Al and Mg alloys have been applied as a promising approach in many cases. The possible extension in applicability requires the enhancement of the mechanical properties and other essential characteristics. It is worth noting that Mg is the lightest among engineering metals for structural applications. Magnesium alloys exhibit also high specific strength, excellent machinability, and the capability to absorb vibrations [35]. Eatson et al. [36] have found a better energy-absorption capacity provided by Mg alloys as compared to Al and steel. The increase in strength and stiffness is required to match technological requirements for use in high demanding applications. Mg alloys are currently applied for use in aerospace according to Federal Aviation Administration (FAA) and SAE Aerospace Standard (AS) AS8049.

However, the low corrosion resistance, the relatively poor mechanical and bulk properties limit the use of Mg alloys in the manufacturing of parts for aircraft. This problem is not solved even after the implementation of ZE41, AZ91, WE43A alloys in the production of gear boxes for helicopters. The commercial casting alloys require the tensile yield strength in the range from 100 up to 250 MPa. The acceptable ductility at room temperature is limited by allowed elongation in the range from 2 up to 8% [37,38].

#### *Classification of Mg Alloys and Applications*

Mg alloys have several alloying elements, such as aluminium, manganese, zinc, silicon, copper, zirconium, and rare-earth metals [2] which tailor the alloys' properties for the selected application. Adding different alloying elements results, in fact, in different alloys properties. One of the most widely used designation systems is the ASTM Standard Alloy Designation System, in which the first two parts identify the alloying content. The role of alloying elements is summarized in [39].

Since corrosion is degradation starting from the surface, the corrosion attack process can be affected by modification and microstructure, by changing the surface composition, or by a combination of these methods. Corrosion of magnesium and magnesium alloys can be minimized by applying conventional barrier coatings or noble materials using a variety of techniques. However, during some coating processes a strong substitution reaction occurs, accompanied by the release of a large amount of hydrogen, which can cause a poor adhesion of the coating to the substrate alloy. Pre-treatment is usually a challenging task for coating magnesium alloys and these technologies usually require high capital investment and energy consumption. Moreover, the corrosion and adhesion properties of these coatings on magnesium are still unsatisfactory.

The present paper is aimed to provide a short review of recent achievements in corrosion protection of magnesium alloys, both surface treatments and coatings, with particular focus on Mg-Al-Mn-Ce, Mg-Al-Zn-Mn and Mg-Zn-Zr alloys, because of their wide application in the transport industry.

## 2. Corrosion of Magnesium and Its Alloys

The main anodic reaction for magnesium in acidic and neutral solutions is that producing  $Mg^{2+}$  ions from pure Mg, whereas, in alkaline solutions, there is the formation of a more or less protective magnesium oxide/hydroxide ( $MgO/Mg(OH)_2$ ). Consequently, magnesium easily corrodes or anodically dissolves in acidic and neutral solutions, combined with the hydrogen evolution, but is capable of being covered and possibly protected by a passivation film during corrosion or anodic polarization in alkaline solutions (Figure 2 and Mg Pourbaix diagram, shown in Figure 3) [40,41].

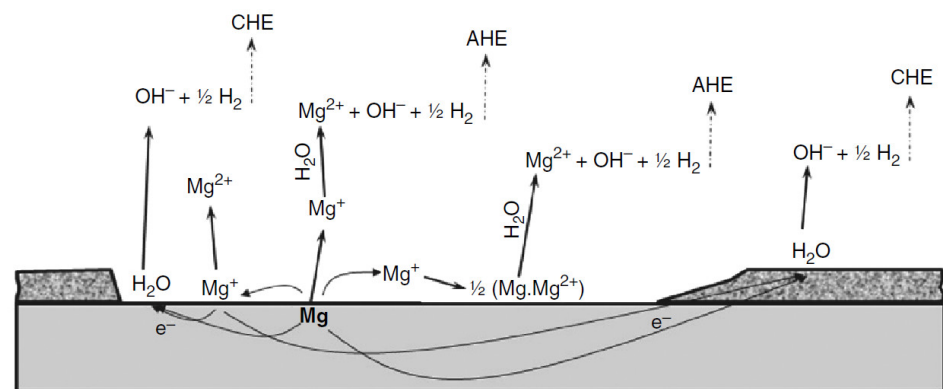


**Figure 2.** Schematic illustration of anodic and cathodic reactions involved in self-corrosion of magnesium. Reproduced from [42] with permission from Elsevier.

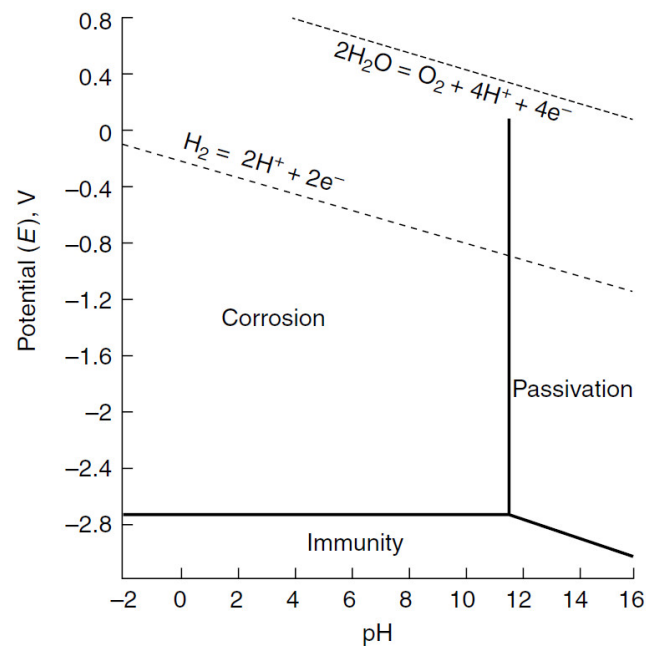


**Figure 3.** Potential-pH diagram (according to Pourbaix) for magnesium and water system at 25 °C showing theoretical areas of corrosion, protection and passivation. Adapted from [41].

There are the following main methods for combating corrosion of magnesium alloys:

- increasing the corrosion resistance of magnesium alloys through alloying with components that help to reduce the rate of corrosion processes;
- application of coatings that enhance the resistance to corrosion and increase the resistance to mechanical action on parts made of magnesium alloys;
- changing the structure of surfaces and parts due to concentrated energetic action (for example, laser ablation).

#### *Influence of the Chemical Composition of Magnesium Alloys on Corrosion Properties*

The corrosion resistance of magnesium and its alloys depends on alloying elements, metallic impurities and non-metallic inclusions (Figure 4).

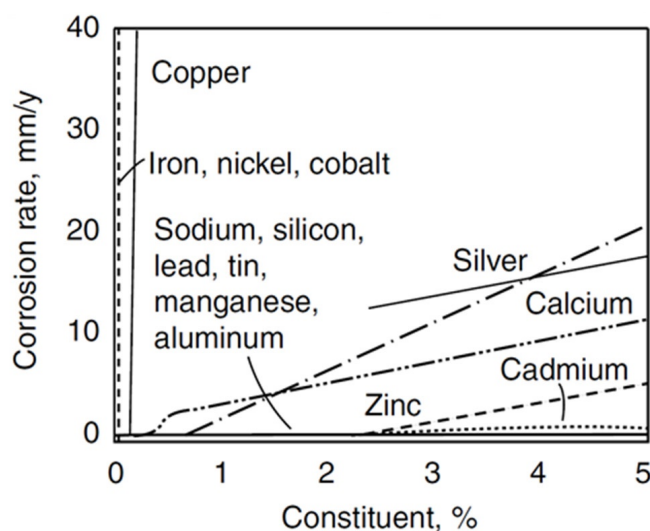


**Figure 4.** Influence of alloying and polluting metals on the corrosion rate of magnesium, determined by alternate immersion in a 3% NaCl solution. Reproduced from [43] with permission from Elsevier.

The increase in the corrosion rate under the influence of metallic impurities and alloying additions is primarily associated with the high overpotential related to hydrogen evolution on magnesium by semi reaction  $2\text{H}^+ + 2\text{e}^- \rightarrow \text{H}_2$ —an evolution of hydrogen, see Table 2.

**Table 2.** Standard electrode potential  $E^0$  at 25 °C for some elements [44].

Reaction	$E^0$ (V)	Reaction	$E^0$ (V)	Reaction	$E^0$ (V)
$\text{Au}^{3+} + 3\text{e}^- \rightarrow \text{Au}$	+1.498	$\text{Sn}^{2+} + 2\text{e}^- \rightarrow \text{Sn}$	−0.138	$\text{Mn}^{2+} + 2\text{e}^- \rightarrow \text{Mn}$	−1.185
$\text{Pt}^{2+} + 2\text{e}^- \rightarrow \text{Pt}$	+1.180	$\text{Mo}^{3+} + 3\text{e}^- \rightarrow \text{Mo}$	−0.200	$\text{Zr}^{4+} + 4\text{e}^- \rightarrow \text{Zr}$	−1.450
$\text{Pd}^{2+} + 2\text{e}^- \rightarrow \text{Pd}$	+0.951	$\text{Ni}^{2+} + 2\text{e}^- \rightarrow \text{Ni}$	−0.257	$\text{Ti}^{2+} + 2\text{e}^- \rightarrow \text{Ti}$	−1.630
$\text{Hg}^{2+} + 2\text{e}^- \rightarrow \text{Hg}$	+0.851	$\text{Co}^{2+} + 2\text{e}^- \rightarrow \text{Co}$	−0.280	$\text{Al}^{3+} + 3\text{e}^- \rightarrow \text{Al}$	−1.662
$\text{Ag}^+ + \text{e}^- \rightarrow \text{Ag}$	+0.800	$\text{Cd}^{2+} + 2\text{e}^- \rightarrow \text{Cd}$	−0.403	$\text{Mg}^{2+} + 2\text{e}^- \rightarrow \text{Mg}$	−2.372
$\text{Cu}^+ + \text{e}^- \rightarrow \text{Cu}$	+0.521	$\text{Fe}^{2+} + 2\text{e}^- \rightarrow \text{Fe}$	−0.447	$\text{Na}^+ + \text{e}^- \rightarrow \text{Na}$	−2.710
$\text{Cu}^{2+} + 2\text{e}^- \rightarrow \text{Cu}$	+0.342	$\text{Cr}^{3+} + 3\text{e}^- \rightarrow \text{Cr}$	−0.744	$\text{Ca}^{2+} + 2\text{e}^- \rightarrow \text{Ca}$	−2.868
$2\text{H}^+ + 2\text{e}^- \rightarrow \text{H}_2$	0.000	$\text{Zn}^{2+} + 2\text{e}^- \rightarrow \text{Zn}$	−0.762	$\text{Li}^+ + \text{e}^- \rightarrow \text{Li}$	−3.040

Therefore, the presence of elements such as Fe, Ni, Co, Cu with low hydrogen overpotential contributes to a sharp increase in the rate of corrosion in environments where the process proceeds mainly with hydrogen depolarization. However, under conditions of oxygen depolarization (atmospheric conditions), all metals significantly experience a reduction in corrosion. The corrosion resistance properties of the alloy can be influenced not only by the main alloying components. Small additives, increase or decrease corrosion resistance properties provided they are uniformly distributed. One of the most effective

resistance to corrosion systems are alloys characterized by the presence of the peritectic Mg-Mn and Mg-Zr. However, the technical features of the Mg-Zr master alloy production allow for the content of  $\text{Cl}^-$  from 0.5 to 2.5 wt%, which can get a negative effect on the anti-corrosion properties of the alloy and should be taken into account when developing the alloy composition [45].

The effect of changes in corrosion resistance under the influence of heat treatment is associated with a change in the phase composition. The presence of intermetallic compounds in the alloy worsens the corrosion resistance since the secondary phases are strong cathodes or self-dissolved at a higher rate. The exception is the alloys of the Mg-Al and Mg-Al-Zn-Mn systems (AZ80A alloys-type). The corrosion resistance of these alloys is higher in the cast and aged states than in the homogenized ones because the  $\text{Mg}_{17}\text{Al}_{12}$  compound is an ineffective cathode and has a high corrosion resistance [45].

The use of chlorine-based fluxes in magnesium casting can cause one of the most dangerous types of corrosion, the so-called “flux corrosion”. The danger is that the inclusions tend to go to the surface, and this often occurs in the depth and generates pores in the metal parts [45]. The most effective method of dealing with flux inclusions is to change the casting technology, when casting under a layer of chloride flux is replaced by casting in a protective gas [46,47].

### 3. State of the Art

The reduction in body weight is a crucial aspect of modern vehicle design. Novel approaches bring the greatest energy and  $\text{CO}_2$  emissions savings in the transportation and maritime sectors [48]. Magnesium is an underestimated high-value-added metal for the aerospace, automotive and marine industry due to low corrosion protection solutions. The critical limits are met in the case of vibration-loaded parts (e.g., wheels and suspensions) in the presence of saltwater. Moreover, flammability is one of the application limiting factors for use in aircraft interiors. Some fundamentals of magnesium ignition and flammability along with laboratory testing procedures and correlations with full-scale fire scenarios, related in particular to the aircraft cabin, have been reported in [36].

Currently, the usage of magnesium in biomedical applications is becoming more and more widespread. The usage of implants made of magnesium alloys as a material for replacing bone tissue has several advantages over implants made of stainless steel, titanium, etc. First of all, magnesium implants are much lighter. The elastic modulus of magnesium alloys, in the range of 41–45 GPa, very closely matches the elastic modulus of bone tissue, which is equal to 3–20 GPa, resulting in the reduction of stress shielding effect that can lead to bone loss around the implant [49]. Magnesium is the most biocompatible material for the use of bone implants and vascular stents. Biocompatibility is determined by several factors: it is known that up to 65% of the total magnesium content in the human body falls on the bone tissue, and excess magnesium cations are effectively naturally removed from the human body. However, the bio-environment is quite aggressive for magnesium alloys and the destruction of the implant can occur earlier than the restoration of bone tissue, therefore it is important to pay attention to the corrosion protection of magnesium-based alloys under the influence of the internal human environment and blood plasma [50]. An insight of magnesium alloys and composites for orthopaedic implant applications is reported in ref. [49].

Alloying, surface coating and surface treatments are considered the most effective ways to prevent corrosion of Mg-based materials [51]. Coatings are essential for corrosion protection because they provide a physical barrier that impedes the access of aggressive species to the metallic substrates and/or inhibits the corrosion process [52–55]. Pure Mg has a very low standard equilibrium potential ( $-2.37$  V vs. standard hydrogen electrode) among all structural metals, which determines the assumption of low corrosion resistivity in humid service conditions for Mg alloys, thus suffering generalized corrosion, galvanic corrosion when coupled with more noble metals as well pitting corrosion [56,57], as a consequence of the environmental conditions.

The global magnesium alloys market size has been valued at USD 1.27 billion in 2019 and is projected to reach USD 3.2–3.4 billion by 2027 at a compound annual growth rate (CAGR) of 11.63–12.3% from 2020 to 2027 [58,59]. Magnesium alloys have a great potential to reduce vehicle weight, fuel consumption, and greenhouse gas emissions in vehicles use life. However, magnesium and some alloying elements are critical raw materials (CRMs) as reported by the European Commission since 2011 [60–63], thus, have high economic importance (EI) and supply risk (SR) for the EU. Many of these elements are also declared as critical minerals in the United States with an absolute or high degree of import reliance: manganese, rare earth elements group, magnesium, zirconium and aluminium [64,65]. Almost 90% of magnesium global production are concentrated in China, as shown in Figure 5. The United States has high import reliance (50%) for magnesium [64] and there is no production of pure magnesium in the EU: entire supply depends on imports from China and a few other non-EU countries (Israel, Russia, and Turkey) [33].

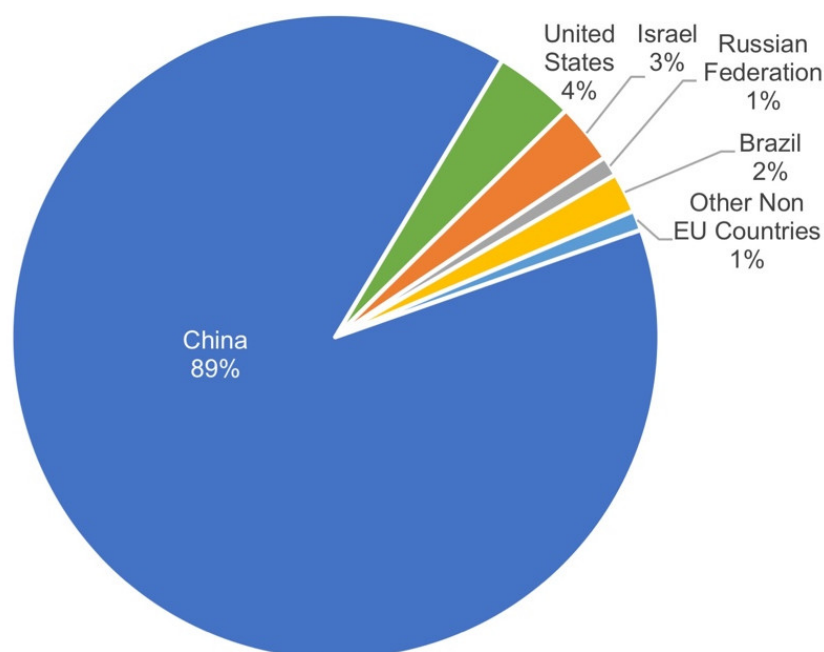


**Figure 5.** The global production of magnesium, in period 2012–2016. Adapted from [33].

The “criticality map” for raw materials assessed by the European Commission and released in 2020 [66], is shown in Figure 6. It should be noted that, since the assessment methodology was revised in 2017, calculations of economic importance and supply risk are not directly comparable with results of the 2011 and 2014 assessments [33]. Magnesium and most commonly used elements in magnesium alloys are marked as critical or non-critical by red and orange colours, respectively. Outstanding properties and advanced applications of magnesium alloys contribute to the high economic importance of all involved elements (surpass EI threshold of 2.8) and high supply risk leads magnesium, silicon, cerium and other rare-earth alloying elements to the list of critical raw materials. Advanced treatment and surface modification of magnesium alloys aimed to mitigate corrosion processes and improve wear performance will extend the lifetime of products, expand the application range for magnesium alloys and effectively contribute to the solutions of critical raw materials problem.

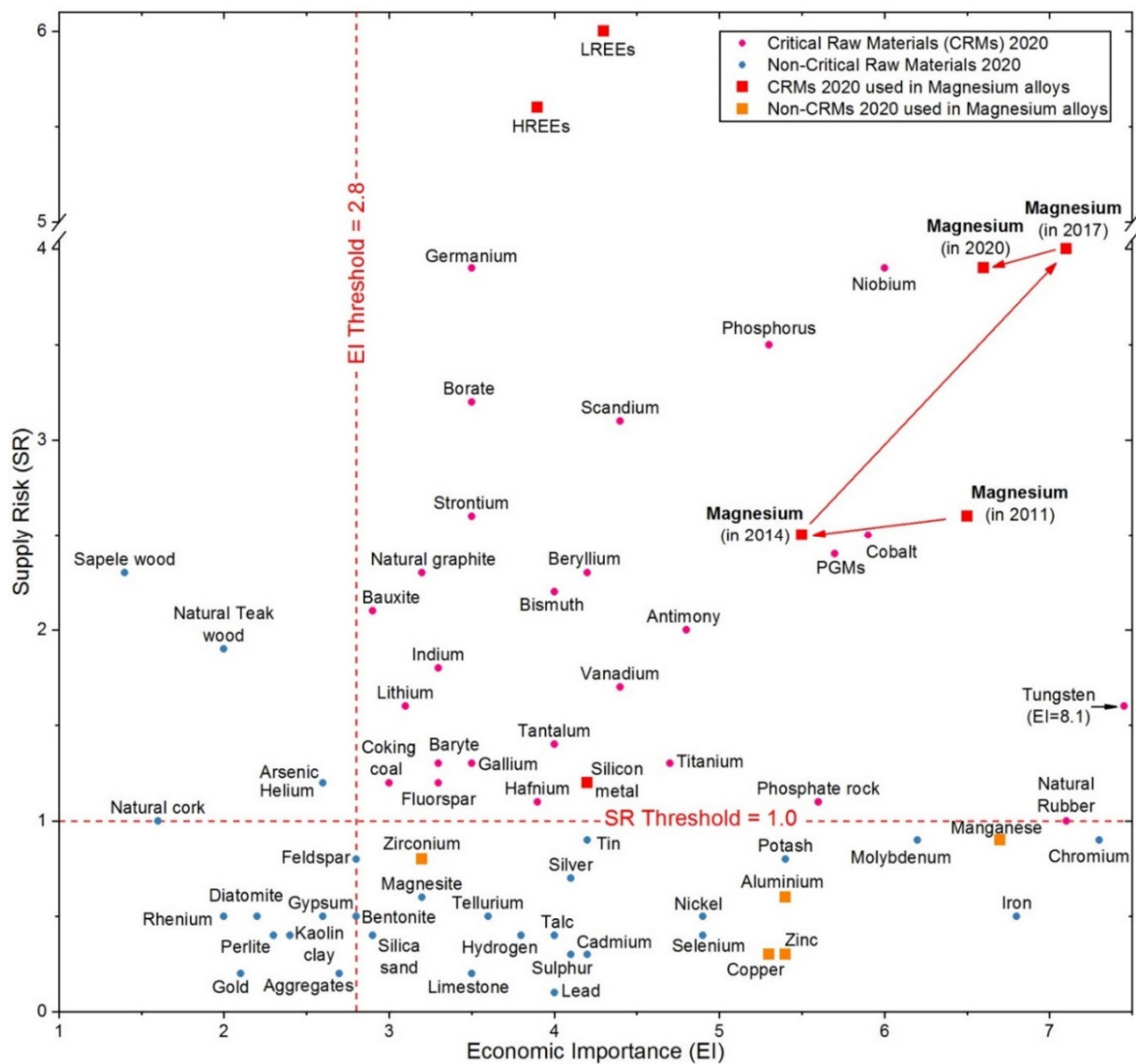


**Figure 6.** Criticality assessment results for raw materials released by the European Commission in 2020 and position of magnesium alloy elements and evolution of magnesium criticality assessment\*. Adapted from [66,67]. \* Since the assessment methodology was revised in 2017, calculations of economic importance and supply risk are not directly comparable with results of the 2011 and 2014 assessments [33].

Since corrosion hinders broader usage of magnesium alloys and limits their application, huge efforts and funds were directed at solving this problem. One of the largest EU research projects directly devoted to the development of anticorrosion coatings for Mg-alloys was “NANOMAG—Development of Innovative Nanocomposite Coatings for Magnesium Casting Protection” launched in 2002–2005 with an overall budget of more than EUR 6.7 million [68]. The general objective was to “develop highly corrosion and abrasion protective coatings by the use of four different optimised coating technologies developed specifically for the different type of applications, for magnesium parts with additional functional properties as demanded by automotive and aerospace industry” [68]. Some of the most notable and publicly available international research projects of the past decade (since the 2010s) addressed to Mg-alloys and corrosion issues are collected in Table 3. However, almost two decades later, the problem of limited use and applications of magnesium alloys due to their significant susceptibility to corrosion is still a great challenge for material science. Although, significant progress in magnesium alloys processing and treatment have been achieved worldwide in recent years [69–77].

**Table 3.** International research projects on magnesium alloys and corrosion issues (selected since 2010).

Acronym or Reference	Project or Consortium Name	Execution Dates (Start and End)	Participating Countries	Overall Budget, kEUR	Ref.
MAFMA Grant agreement ID: 795658	Multiscale Analysis of Fatigue in Mg Alloys	1 September 2019–15 September 2021	Spain	170.1	[78]
SYNPROMAG ANR-18-ASTR-0016	Synergistic Corrosion Protection for Magnesium Alloys	December 2018–June 2021	France	245.9	[79]
ALMAGIC Grant agreement ID: 755515	Aluminium and Magnesium Alloys Green Innovative Coatings	1 June 2017–31 May 2019	Spain, The Netherlands, Germany	999.5	[80]
MAGICOAT POCI-01-0145-FEDER-016597	Controlling the Degradation of Magnesium Alloys for Biomedical Applications Using Innovative Smart Coatings	1 May 2016–31 December 2019	Portugal, Germany	192.9	[81]
LIFE CRAL LIFE15 ENV/IT/000303	Industrial Pilot Plant for Semisolid Process Route with Eco-Compatible Feedstock Materials	1 July 2016–31 December 2019	Italy	3227.3	[82]
MAGPLANT Grant agreement ID: 703566	Localized Corrosion Studies for Magnesium Implant Devices	1 September 2016–31 August 2018	Germany	159.5	[83]
SMARCOAT Grant agreement ID: 645662	Development of Smart Nano and Microcapsulated Sensing Coatings for Improving of Material Durability/Performance	1 January 2015–31 December 2018	Portugal, Germany, Latvia, Czech Republic, Belarus	900.0	[84]
MULTISURF Grant agreement ID: 645676	Multi-Functional Metallic Surfaces via Active Layered Double Hydroxide Treatments	1 January 2015–31 December 2018	Germany, Portugal, Belarus	648.0	[85]
REMAGHIC Grant agreement ID: 680629	New Recovery Processes to Produce Rare Earth-Magnesium Alloys of High Performance and Low Cost	1 September 2015–31 August 2018	Spain, Germany, Belgium, Italy, Cyprus	3709.2	[86]
MARCO POLO Project RAPID	Magnésium Résistant Corrosion Peinture Optimisée Liant Organique	1 May 2014–27 April 2017	France	no info	[87]
ECOPROT ECO/12/333104	Eco-Friendly Corrosion Protecting Coating of Aluminium and Magnesium Alloys	1 November 2013–30 April 2016	Spain, France	1337.6	[88]

Table 3. Cont.

Acronym or Reference	Project or Consortium Name	Execution Dates (Start and End)	Participating Countries	Overall Budget, kEUR	Ref.
COMAG Grant agreement ID: 297173	Development and Implementation of Conductive Coating for Magnesium Sheets in A/C	1 February 2012–31 July 2014	Israel	160.0	[89]
MAGNOLYA Grant agreement ID: 307659	Advanced Environmentally Friendly Chemical Surface Treatments for Cast Magnesium Helicopter Transmission Alloys Preservation	1 September 2012–31 August 2013	Spain, France	200.0	[90]
CO-PROCLAM Grant agreement ID: 270589	Corrosion Protective Coating on Light Alloys by Micro-Arc Oxidation	1 April 2011–31 March 2013	France	399.2	[91]
MAGNIM Grant agreement ID: 289163	Tailored Biodegradable Magnesium Implant Materials	1 October 2011–30 September 2015	Germany, Czech Republic, Belgium, Austria, Sweden, Finland	3129.8	[92]
PTDC/CTM-MET/112831/2009	Fault-Tolerant Anticorrosion Coatings for Magnesium Alloys	1 March 2010–31 August 2014	Portugal, Germany	137.0	[93]
ENABLEG Grant agreement ID: 262473	Environmentally Acceptable Pretreatment System for Painting Multi Metals	1 October 2010–30 September 2012	Sweden, Italy, Spain, Denmark	1064.0	[94]
MUST Grant agreement ID: 214261	Multi-Level Protection of Materials for Vehicles by “Smart” Nanocontainers	1 June 2008–30 September 2012	Germany, Portugal, Norway, Greece, Switzerland, Poland, Italy, Finland, Belgium	10,511.0	[95]
AMD-704	Development of Steel Fastener Nano-Ceramic Coatings for Corrosion Protection of Magnesium Parts	October 2007–30 September 2011	United States	884.0	[96]

Anti-corrosion coatings include conversion coatings, anodization, electroless/electroplating, organic coatings, laser surface treatment, PVD and CVD, thermal/cold spray, etc. In reference. Wang et al. [51] report about different strategies to mitigate corrosion issues in Mg alloys, as reported in the literature. Authors investigated the publications about different coating technologies during the last 20 years and found that chemical conversion coatings, anodizing, plating, and organic coatings seem the most widely investigated methods to improve the corrosion resistance of Mg alloys [51]. In 2011, Wu and Zhang [97] reported on a study based on analysing patented coatings for corrosion and protection of Mg alloys, finding that only a small amount of the analysed patents were exploited at the industrial level.

### 3.1. Currently Applied Coating Solutions for Magnesium Alloys

#### 3.1.1. Hexavalent Chromium ( $\text{Cr}^{+6}$ ) Based Systems

$\text{Cr}^{+6}$  is a known carcinogen species. Its use rapidly declined or due to stricter permissions, restrictions or even banning legislations. The growing number of alternative chemical treatment systems rapidly replaced the  $\text{Cr}^{+6}$ . For example, the  $\text{Cr}^{+6}$  is banned in China, it does not match the Restriction of Hazardous Substances (RoHS, EU) Directive 2002/95/EC and the United States restricts its application to legacy programs and military industry.

Several alternatives to hexavalent chromium conversion coatings (CCC) have been proposed. Organosilane compounds, having the general formula  $\text{R}_n\text{SiX}_{4-n}$  (where X is the hydrolyzable group and R is an organofunctional group), are extensively investigated. These compounds show good corrosion protection properties when are deposited on different types of metal substrates: they form a barrier constituted by Si-O-Si networks forming stable chemical bonds with the surface of metals [98]. Silane-based anticorrosive coatings of Mg alloys have been proven to be effective, economical and environmentally friendly [98]. A review of recent advancements in corrosion protection of magnesium alloys by silane-based sol-gel coatings are reported in [99]. The addition of corrosion inhibitors may further increase their corrosion resistance [99]. Organosilane coatings will be more widely discussed in the next Section.

Several Cr-free CCC of different nature were proposed for Mg alloys, such as phosphate-permanganate, fluoride and stannate [99,100]. A review of corrosion resistance conversion coatings for Mg and its alloys is reported in ref. [100]. The state of the art of Cr-free coatings solutions is summarized below.

#### 3.1.2. Phosphate(s) Based Systems

Primarily, they are used on iron and zinc-based substrates, as an alternative to  $\text{Cr}^{+6}$  CCC systems, after a chemical cleaning process that prepares the surface for the phosphate treatment. Fair to good topcoat adhesion results with a minimal corrosion resistance when used as a stand-alone treatment with 24–48 h of salt spray test (SST) exposure before the appearance of corrosion products. Phosphate systems are coming under increasing environmental scrutiny as a result of the wastewater treatment and the fact that phosphates are one of the primary causes of eutrophication—the response of the ecosystem to the addition of artificial or natural substances, such as nitrates and phosphates, through fertilizers or sewage to an aquatic system causing a loss of oxygen in the water system.

#### 3.1.3. Zirconization

Developed in the mid to late nineties. The process is “relatively” new, but it makes significant inroads in displacing phosphate-based systems bringing many benefits when applied to various substrates. At this time there is limited data concerning the application of this process on Mg-based alloys; however, results obtained when it is applied on Al-based alloys supply resistance to SST of 48–96 h and magnesium would likely perform with similar results.

### 3.1.4. Anomag

Anodization of magnesium has been available using a Cr<sup>+6</sup> DOW17 process and a non-chromium process DOW hard anodizing surface coating process (HAE) that provided a superior corrosion resistance and paint adhesion than the traditional Cr<sup>+6</sup> CCC. The Anomag process uses an electrolytic bath process where the electrolyte contains phosphate and ammonium salts that create a Cr<sup>+6</sup>-free layer on the substrate.

### 3.1.5. Henkel MgC

Trade named by Henkel as Bonderite-MgC, is a plasma electrolytic ceramic deposition process that contains three steps: in the first and second the part is immersed in pre-treatment tanks for surface activation and in the third step, the part puts in charged tank where part get a build-up on the substrate. This process has been in development for three to four years and several projects are entering serial production very soon. This process is similar to Anomag and Keronite but has a lower operating cost.

### 3.1.6. Tagnite and Keronite

These are additional plasma electrolytic oxidation (PEO) processes that are produced in an alkaline aqueous solution containing hydroxide, fluoride and silicate species with no chromium or other heavy metals, and provide another level of paint adhesion and corrosion resistance beyond Anomag. At the moment, this process supplies the best coating solutions for Mg alloys. These treatments are typically used in defence, aerospace, elite sports and very high-end applications. However, according to reports, these coatings are not resistant to intensive vibration and fail automotive and marine corrosion tests. It is possible to explain this fact by the presence of a ceramic layer—MgO (magnesium oxide) which has a “porous-like structure”. The main drawback of the MgO layer is ascribable to its hydrophilicity and hygroscopicity, which are critical characteristics for long-term protection. An additional crucial drawback of the MgO is that it has a “fragile” structure with a low resistance to vibration (in particular, during long-time exposure) making this type of coating not suitable for the marine and automotive industry. The PEO process will be more widely described in Section 6.

Summarizing: it is well-known that Cr-based CCCs are good against corrosion but, in the last decades, all research moved to replace them through other solutions/systems, due to Cr<sup>6+</sup> in a chromate bath is a highly toxic carcinogen and is being phased out. The development of an environmentally friendly process [101] is necessary due to the increasingly stringent environmental legislation nowadays

## 4. Organic/Polymer Coatings

Organic (polymer) coatings are a widely used type of the coatings for protection of magnesium alloys, typically as final or top coating [51,102]. The organic coating can provide simultaneously corrosion protection and decorative appearance. Furthermore, organic coatings, after appropriate pre-treatment and/or post-treatment might have superior adhesion, abrasion, wear, superhydrophobic properties and self-healing properties [73,103,104].

Usually, an organic coating consists of (1) a layer of binder or vehicle, (2) pigments and (3) different additives such as dryers, hardening agents, stabilizing agents, surface activating compounds, and dispersion agents [103]. Additionally, polymer coatings might contain corrosion inhibiting chemicals which further improve the protection effect.

Surfaces should be free of contaminants, oxides and other foreign or released substrate particles, furthermore, all trapped moisture or air in surface pores must be removed before covering with coating [104]. The cleaning process typically acts in two ways: (1) remove all contamination from the surface, and (2) roughen the surface to increase the adhesion of a coating.

Typical cleaning consists of mechanical treatment, cleaning with solvents, alkaline treatment and pickling or etching.

Processes used for applying organic coatings involves a wide variety of techniques, such as painting, powder coating, cathodic electrocoating (E-coating), sol-gel coating, polymer plating, plasma polymerization and the application of lacquers, enamels and varnishes [51,73,102,104–106]. The overview of the most widespread organic coatings applying processes is given in Table 4. It should be noted that any of the described processes have different advantages and disadvantages which relate to the solvent used. In the past, numerous used solvent bases represented a significant concern to the environment or humans. However, in recent years alternative processes which eliminate this problem are more readily available, like different powder coatings (no solvents) or the use of compliance solvents (e.g., waterborne solvents).

**Table 4.** Overview of organic coatings applying processes [51,102].

Process	Description of Process	Advantages	Disadvantages
Painting	The usual composition of paint is resin, solvent, pigment and additives. The selection of an alkali-resistant primer (resin) such as acrylic, polyvinyl butyral, polyurethane, vinyl epoxy or baked phenolic is one of the most important steps in the painting of Mg alloys. The painting film is usually formed by evaporation of the solvent or by some chemical reactions.	Flexibility, ease of cover of work pieces with complex geometry.	Use of organic solvent, multistep.
Powder coating	The thermoplastic powders are applied by techniques such as electrostatic powder spraying or flame spraying to the Mg substrate. After deposition, powders are heated to fuse the polymer in a uniform, pinhole-free film.	Utilisation of no solvents, environmentally friendly; low hazards of flammability/toxicity and energy consumption. Achieved in a single operation with almost 100% powder utilisation.	The powders are stored in pulverised form and have to be very dry. Difficult to obtain thin coatings; difficult to coat depressed areas. The high diffusion temperature.
E-coating	The E-coatings (electrophoretic coating) are formed by the precipitation of charged particles from a liquid to the charged Mg alloy substrate surface in an electric field.	Short formation time; simple equipment; automatic processing; high coating material use; evenly coating thickness; small restriction on the substrate shape; no requirements for binder burnout.	Complex electrical control and maintenance of bath solution; thickness usually in a range from 10 to 30 µm; obvious roughness of the substrate.
Sol-gel coating	The sol-gel coatings are formed through gelation of a colloidal suspension, involving: hydrolysis, condensation polymerisation of monomers to form particles, agglomeration of the polymer structure, and final heat treatment.	Low process temperature; possible to form coatings on complex shapes and to obtain thin films. Waste-free and eliminates the need for a washing stage.	Demands a long-time process flow; phase separation during curing; crack formation due to stresses developed during drying and thermal treatment; limited thickness.
Polymer plating	Polymer plating is the electrochemical polymerisation of a polymer film on the surface of a substrate that functions as one of the electrodes in the electrochemical cell.	A minimum number of pre-treatment steps were required.	Limited data on long term properties, this process is still in its infancy.
Plasma polymerisation	Polymeric coatings can be applied from the gas phase by exposing a substrate to a reactive gas in the presence of a glow discharge plasma.	The thin uniform coating on the surface.	Limited data on corrosion resistance in salt-spray conditions. Not suitable for harsh service conditions

According to Wang et al. [51], powder coating and E-coating have been recognized as the two most popular organic coatings for the protection of magnesium components against corrosion in the automotive industry. The powder coating provides better general and galvanic corrosion resistance, while E-coating has lower cost, it is not a line-of-sight coating technology, therefore allowing good coverage also of components with complex geometries. Commercially offered solutions for powder coating are products of ProTech, Akzo/Interpon and DuPont, while E-coatings are offered by PPG, BASF, and DuPont [51].

The primary component of an organic coating is resin, which can be of several variants, as epoxy, polyvinyl butyral, vinyl, acrylic polyurethane, and baked phenolic with added zinc chromate or strontium chromate [102]. The layer of coatings should be uniform,

pore-free, well adhered to the substrate and self-healing to achieve desired protection of magnesium alloy. The self-healing can be accomplished by the presence of corrosion inhibiting pigments or by different additives in the coating [73]. In a harsh and challenging environment, sometimes a multiple-layer coating system made of a primer, several midcoats and topcoat is necessary. By use of different treatment processes and coating compositions a variety of decorative effects can be achieved on magnesium alloy, such as: bright metal (buff + ferric nitrate pickle + clear epoxy or acrylic); satin finish (wire brush or pickle + ferric nitrate + clear epoxy or acrylic); tinted clear (ferric nitrate pickle + tinted epoxy or acrylic); metallic (chrome pickle or dilute chromic acid + epoxy, acrylic, polyvinyl butyral or vinyl pigmented with metal powder or paste); textured leatherette (chrome pickle or dilute chromic acid + vinyl organosol); and others [104].

#### *Application Examples*

Lamaka et al. [107] have developed and tested a new anticorrosion protection coating for magnesium alloy ZK30 (Mg-Zn-Zr). The protective coating is based on an anodic oxide layer loaded with corrosion inhibitors with  $Ce^{3+}$  and 8-hydroxyquinoline in its pores, which is then sealed with a sol-gel hybrid polymer composed of titania nanoparticles and (3-glycidoxypropyl)-trimethoxysilane (GPTMS). The porous oxide layer is produced by spark anodizing and it enables good adhesion of the sol-gel film as it penetrates through the pores and forms an additional transient oxide-sol-gel interlayer. The produced protective coating has a thickness of about 3.7–7.0  $\mu m$ . The blank or  $Ce^{3+}$  ions doped oxide-sol-gel coating system proved to be an effective corrosion protection for the magnesium alloy ZK30 preventing corrosion attack after exposure for a relatively long duration in an aggressive NaCl solution.

Zhang and Wu [105] in their overview of submitted patents regarding organic coatings on magnesium alloys, noticed that silane application plays an important role in new technological patents. Silane is a type of environmentally friendly organic/inorganic hybrid, with a high potential to replace toxic chromates. It is a hydrolysable alkoxy group such as methoxy ( $-OCH_3$ ), ethoxy ( $-OC_2H_5$ ), acetoxy ( $-OCOCH_3$ ). It has a general formula of  $R'(CH_2)_nSi(OR)_3$ , where  $R'$  represents an organofunctional group, which bonds well with paint. The silane film cannot be applied individually as it is too thin to protect the magnesium alloys for a long time. However, it can be an excellent paint primer, providing good topcoat adhesion to the metal.

Tong et al. [108] demonstrate the formation and properties of new graphene oxide (GO) coating fabricated on the surface of extruded Mg-Zn-Ca alloy (Mg-5.7Zn-0.8Ca), by the silane coupling agent. The surface was fully covered by a two-step process: (1) silane layer was formed by immersion in 5% silane, 5% deionised water and 90% ethanol solutions at room temperature for 2.0 h, and then cured at 100 °C for 0.5 h; (2) silanized Mg substrate was kept in graphene oxide dispersion at ~40 °C for 24 h, and then dried at 80 °C for 1.0 h. The formed GO coating fully covered the substrate by the chemical reactions and formed a multilayer overlapped structure due to the interlocking effect. The anti-corrosion properties were greatly improved by silane/GO coating, as the stable covalent bonds in the coating successfully limit the infiltration of electrolyte into the Mg surface due to barrier formation. The GO coating possesses high hardness and lubrication due to the superior bonding between the Mg substrate and GO sheets and thus resulting in excellent wear resistance. Furthermore, it was concluded that the GO coating is a simple, cost-effective and environmentally friendly class of the Mg surface coating process.

Sang et al. [109] shown that a polymeric nano-film on the surface of Mg-1.5Mn-0.3Ce alloy produced by polymer plating of 6-dihexylamino-1,3,5-triazine-2,4-dithiol monosodium (DHN) significantly improves Mg alloy corrosion resistance. The surface is modified from hydrophilic into hydrophobic with the increase of water contact angle of 45.8° to 106.3°. The polymeric film increased the corrosion potential from  $-1.594$  V vs SCE for blank to  $-0.382$  V vs SCE, while the charge transfer resistances increase was from 485  $\Omega cm^2$  of

blank surface to  $2.717 \Omega\text{cm}^2$  for polymer plated. Hence, the polymer-plated Mg-Mn-Ce surface with hydrophobic characteristics has excellent anti-corrosion properties.

Fang et al. [110] investigated enhanced properties of silk fibroin/sodium alginate composite coatings on biodegradable Mg-Zn-Ca alloy (Mg-2Zn-1Ca). As magnesium alloy Mg-Zn-Ca is biodegradable an appropriate polymer coating with superb biocompatibility is necessary to solve the local alkalinity and rapid hydrogen release. In this case, natural organic silk fibroin could be used, however, the adhesion and mechanical properties should be achieved without any chemical conversion/intermediate layer. For that, based on VUV/O<sub>3</sub> surface activation, a hybrid of silk fibroin and sodium alginate is used on hydrophilic Mg-Zn-Ca alloy surfaces. It was found that a mass ratio of 70/30 of silk fibroin/sodium alginate was necessary for the optimum coating. The adhesion force was tripled, while mechanical properties were significantly improved when compared to pure silk fibroin and/or sodium alginate coatings. Furthermore, the corrosion rate of the coated Mg alloy was significantly delayed.

Kartsonakis et al. [111] evaluated a corrosion resistance of magnesium alloy ZK10 (Mg-1.4Zn-0.55Zr) coated with the hybrid organic-inorganic film including containers. Coatings consisted of cross-linked polymers (bisphenol a diglycidyl ether based) and containers consist of cerium molybdate loaded with 2-mercaprobenzothiazole (MBT) corrosion inhibitors. These coatings performed improved corrosion protection properties after exposure to 0.5 M NaCl solution for 4 months. In the case of artificial defected coatings immersed in 1 mM NaCl solution for 73 h, a partial self-recovery of the films is noticed. The incorporation into the films of containers loaded with corrosion inhibitor MBT enhanced the self-healing effect due to the increase of the charge transfer resistance.

Liu and Kang [112] prepared two kinds of hydrophobic organic ultrathin films on the surface of Mg-Mn-Ce (Mg-1.5Mn-0.3Ce) alloy by two different organic compounds with the same terminal group octadecyl. The OTS film was prepared by self-assembling of the n-octadecyl trichlorosilane (OTS), and STN film was prepared by polymer-plating of octadecyl compound 6-stearyl amino-1,3,5-triazine-2,4-dithiol monosodium (STN). The adhesion force at the nano scale was reduced from 12.35 nN for the substrate to 5.76 nN for STN film and 4.12 nN for OTS film. Thus, the wettability of the Mg-Mn-Ce surface transformed from hydrophilicity to hydrophobicity. Furthermore, the nano friction force and coefficient were also effectively reduced.

## 5. Multiple Surface Coatings

To achieve a satisfactory corrosion protection effect with desired mechanical properties multilayer coating systems are necessary [51,102,104–106]. In practice, these kinds of systems are extensively used, and they incorporate different layered coatings produced from different materials, often utilising different technologies (electrochemical plating, conversion coatings, anodizing, gas-phase deposition processes, organic/polymer coatings, electrolytic plasma oxidation, etc.). Typically, multilayer surface treatment has consisted of chemical conversion or anodizing followed by top paint (organic) coating. The chemical conversion or anodizing film can improve not only the adhesion between Mg substrate and paint coating but also the corrosion resistance of the organic coating. The use of multilayer systems does not have just the benefit of adding (stacking) different properties, but multiple layers have an additionally synergistic effect on the corrosion properties of the coating.

As an illustration of different possibilities of multilayer system a schematic representation of typical multilayer coating system in the automotive industry (chemical conversion produced chromate first layer, and several organic layers applied by painting) [51,102], and composite hydroxyapatite-polytetrafluoroethylene (PTFE) coating on biomedical Mg-Zn-Ce alloy [113] is shown in Figure 7.

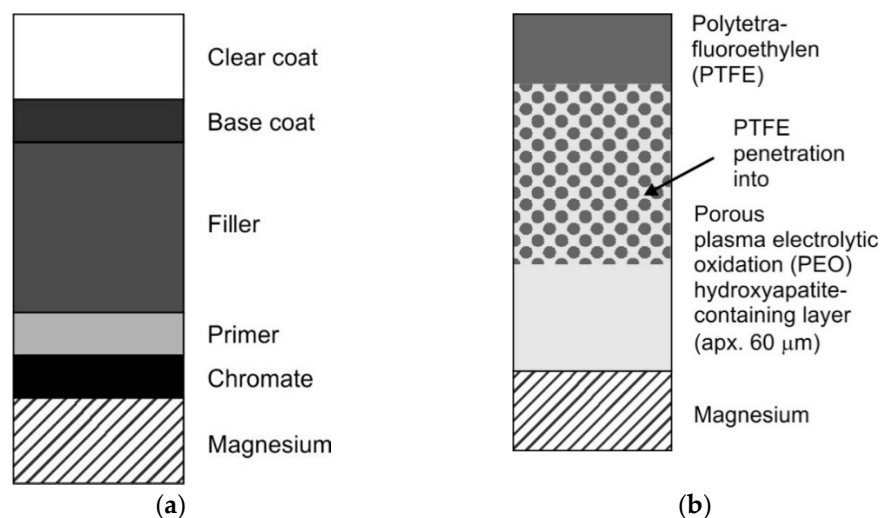


**Figure 7.** Schematic representation of typical multilayer coating system: (a) Automobile Mg part coating (chromate first layer, and several organic layers) [114]; (b) Composite hydroxyapatite—PTFE coating on Mg-Zn-Ce alloy [113].

Different interesting multilayer systems have been overviewed by Zhang and Wu [106]. They have highlighted several examples like the formation of an insoluble  $MgF_2$  film on the surface, followed by immersion of the coated metal in an aqueous solution of alkali metal silicate and an aqueous solution of alkali metal hydroxide (US patent 4184926). In this way, a two-layer coating is formed with increased corrosion and abrasion resistance due to  $MgF_2$  film and topcoat anodizing coating. It is also more resistant to strong acids and alkali. In another example: firstly an oxide film is formed by anodic oxidation; then a coat of a thermosetting resin film is formed; and finally a metallic conductive film is formed by a vapour deposition method (DE patent 19853576834, US patent 41124389A, JP patent 59215110). This three-layered system enhances corrosion resistance and conductivity. The third example (JP patent 2005325416) represents a four-layer structure consisting of nickel/copper/aluminium layers which were plated successively on magnesium alloy, with the fourth layer of an anodized aluminium coating on the outer surface. In this way, the internal stress generated between outer layers relaxed by a copper plating film between them, thus improving the adhesion of the layers.

## 6. Plasma Electrolytic Oxidation

The method of plasma electrolytic oxidation (PEO) [115,116] (for Mg-Mn and Mg-Zn alloys [117–119]), also known as microarc oxidation (MAO), refers to protective coatings for magnesium and other light alloys formed in electrolytes as a result of plasma electrolytic reactions when an electric current is applied. PEO process is aimed to increase corrosion and wear resistance properties of the substrate material. PEO is a combination of the uniformity of an electrolytic process with an intense local injection of energy (through the local discharges—a micro-arcs). The coatings formed by the PEO method have generally good adhesion to the substrate and low porosity. In the case of Mg alloys, PEO coating is a magnesium oxide-based coating. Depending on the electrolytes used, i.e., silicate, alumina, phosphate base electrolytes, different products are formed together with  $MgO$ .  $Mg_2SiO_4$  and  $MgO$  are the main phases formed during coating in a silicate based electrolyte, while,  $MgO$  and  $Mg_3(PO_4)_2$  are formed in a phosphate based electrolyte [120,121]. Figure 8 shows as an example, the XRD diffraction patterns of a MA8 alloy coated by PEO in a silicate base electrolyte [122].

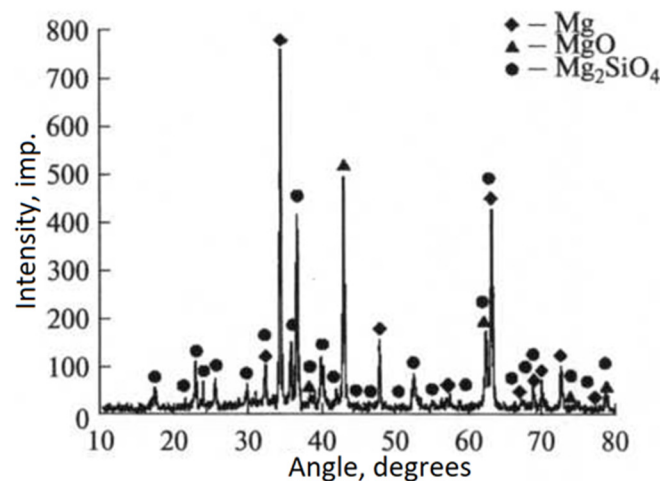


**Figure 8.** Diffraction pattern of the surface of a sample of magnesium alloy MA8 (Mg-2.0Mn-0.25Ce) with a coating formed by the PEO method in a silicate base electrolyte. Adapted from [122].

Using the PEO process it is possible to obtain cheap coatings with an interesting combination of properties. For example, the group of Prof. Zinigrad conducted research of PEO of high-strength creep resistance magnesium alloys produced by Dead Sea magnesium [123,124].

To form the coating by the PEO method, an alkaline solution was used, consisting of 12 g/L of  $\text{Na}_2\text{SiO}_3 \cdot 9\text{H}_2\text{O}$ , 5 g/L of NaF, 2 g/L of  $\text{K}_2\text{TiF}_6$ , 3 g/L HA nanoparticles (20 nm) and 10 mL/L ethylene glycol. The pH level = 12 was corrected by using a NaOH solution [125].

The distribution of chemical elements that make up the electrolyte is the same for most magnesium alloys, which indicates the versatility of this method.

The work [117] shows the results of a study of the effect on the corrosion resistance of various magnesium alloys, the surface of which was processed by the PEO method in bipolar mode. In the anode mode, the voltage increased from 30 to 300 V at a rate of  $45 \text{ V} \cdot \text{s}^{-1}$ . In the cathodic mode, the voltage was fixed at 30 V. The frequency of polarising pulses was 300 Hz. The anode/cathode period ratio was 1. Table 5 shows the results of studying the alloys MA8 (Mg-2.0Mn-0.25Ce) and MA14 (ZK60) [117].

**Table 5.** Comparison of electrochemical parameters ( $E_{\text{corr}}$ —free corrosion potential,  $i_{\text{corr}}$ —free corrosion current,  $R_{\text{loss}}$ —polarization resistance and  $|Z|_{f=0.01}$ —alternating current polarization resistance) of samples without coating and with PEO coatings [117].

Type of Sample		$E_{\text{corr}}$ (V)	$i_{\text{corr}}$ ( $\text{A} \cdot \text{cm}^{-2}$ )	$R_{\text{loss}}$ ( $\text{Ohm} \cdot \text{cm}^2$ )	$ Z _{f=0.01}$ ( $\text{Ohm} \cdot \text{cm}^2$ )
MA8	Without cover	−1.56	$7.7 \times 10^{-5}$	$4.9 \times 10^2$	$6.3 \times 10^3$
	PEO coating	−1.53	$2.8 \times 10^{-7}$	$9.5 \times 10^4$	$7.5 \times 10^4$
MA14	Without cover	−1.5	$2.3 \times 10^{-4}$	$1.2 \times 10^2$	$2.5 \times 10^2$
	PEO coating	−1.42	$4.1 \times 10^{-9}$	$6.4 \times 10^6$	$4.7 \times 10^6$

When studying the distribution of chemical elements in the coating it was found that the zirconium contained in alloy system Mg-Zn-Zr (ZK60A) is not included in the coating composition due to the high affinity with zinc to form intermetallics  $\text{ZrZn}_2$ ,  $\text{Zr}_3\text{Zn}_2$ , and with hydrogen to form highly dispersed hydrides  $\epsilon\text{-ZrH}_2$ ,  $\delta\text{-ZrH}$ . Over 50% of all introduced zirconium is associated with these phases, and the rest is dissolved in an  $\alpha$ -solid solution based on magnesium, which explains the absence of zirconium in the composition of the surface oxide film. However, PEO-layers formed on alloys containing zirconium—have the best corrosion properties (Table 5). For example, the coating of alloys

of the Mg-Mn-Ce system has the lowest corrosion resistance. Zr forms stable intermetallic compounds in the magnesium alloys, the zirconium oxide may therefore find smiling only in a thin (less than 0.1 mm) layer in between the coating and the substrate. Therefore, the presence of Zr is extremely difficult to detect [126].

In general, PEO coatings not only provide corrosion protection but also improve the mechanical properties, i.e., reduce the friction coefficient and increase the hardness of the surface independently from the starting alloy composition.

It was found that the use of a current with a sequence of pulses “positive-negative” led to the predominance of a “surface” layer with a high concentration of defects and a partial absence of a finely porous transition layer (Figure 9) [127]. Such a structure should negatively affect the protective properties of the coating. The opposite pattern was observed using a polarizing current pulse to the sequence “negative-positive”: the dimensions of the surface and base layers are the same and the boundary between them is visible [128–133]. With this formation of pulses, the volumetric porosity is 11%, and with the sequence “positive-negative” 15%, this is very important since it is the layer with the absence of pores that determines the corrosion protective properties [127].

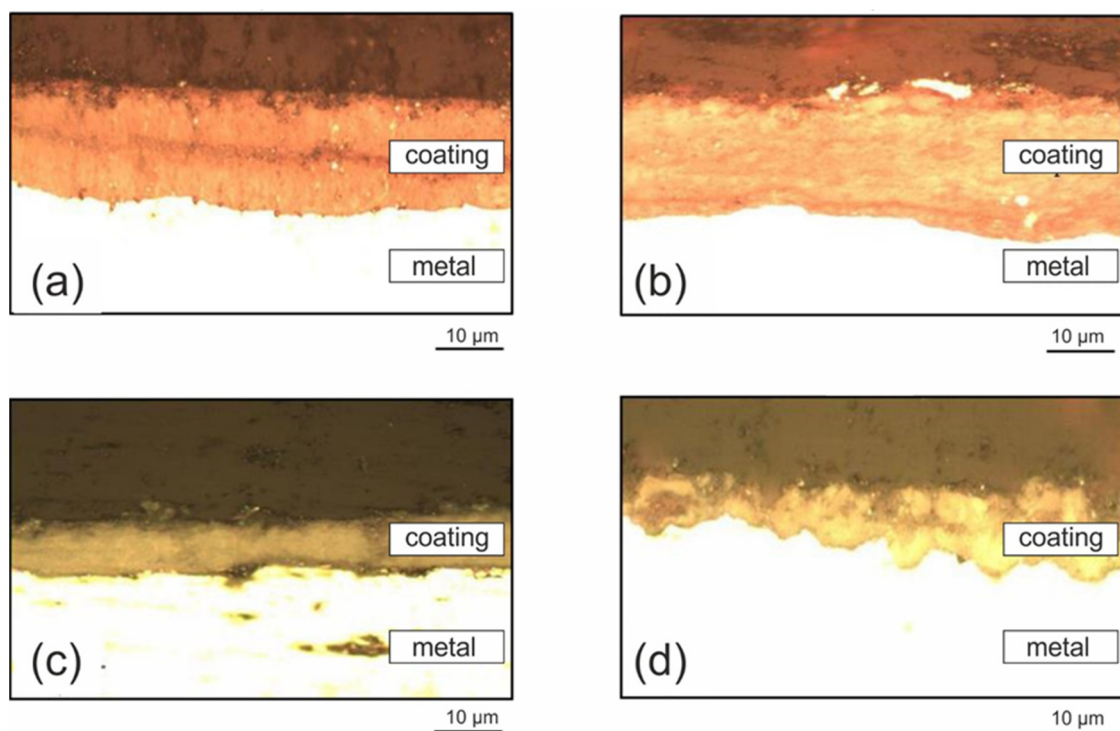


**Figure 9.** Microstructure of coatings obtained by different current modes, with the with the following pulses “negative-positive” (a,c) and “positive-negative” (b,d). Adapted from [127].

The scratch test data showed that the level of antifriction properties was about 3.5 grooves higher than that of the samples not treated with PEO. This makes it possible to expand the field of application of magnesium alloys in conditions where the product can be used both in an environment with an aggressive atmosphere and in conditions of mechanical stress.

#### *Additional Processing of Coatings Applied by Plasma Electrolytic Oxidation*

As mentioned earlier, the disadvantage of coatings deposited by the PEO method is the surface porosity, the formation of which is due to the processes occurring during the coating by this method. The solution to this problem can be an additional treatment with polymers, for example, polyvinylidene fluoride (PVDF) [130,134]. Despite the low cost

among other fluoropolymers, this coating has several advantages, such as high anti-friction properties, resistance to chemical attack, thermal stability and biocompatibility.

The most interesting result is described in [134] which describes the increase of corrosion protection and tribological properties of Mg alloys by using a PVDF layer on a PEO coating. For the study, an alloy of the Mg-Mn-Ce system was chosen, which showed rather weak results when coating by the PEO method. An electrolyte of the following composition was used to apply a protective layer by the PEO method: 15 g/L of  $\text{Na}_2\text{SiO}_3$  + 5 g/L of NaF. To form the PVDF layer a solution of a powder polymer and  $(-\text{C}_2\text{H}_2\text{F}_2)_n$ - and N-methyl-2-pyrrolidone ( $\text{C}_5\text{H}_9\text{NO}$ ) was used. The samples were dipped for 10 s.

The analysis of tribological parameters showed that a single application of the polymer to the PEO layer increases the wear resistance of the coatings by almost two times (Table 6). An increase in the frequency of application up to 2–3 times leads to a significant increase in the number of abrasion cycles to metal (more than 25 times). Cyclic tests were carried out in the following modes: Corundum ball diameter—10 mm; rotation speed— $50 \text{ mm}\cdot\text{s}^{-1}$ ; load—10 N. The best adhesion characteristics are possessed by polymer containing PEO coatings formed by three times application of the polymer. Because exfoliation of the coating is observed at a load equal to  $18.2 \pm 0.2 \text{ N}$ , and penetration of the indenter to the metal at  $18.8 \pm 0.3 \text{ N}$  [134].

**Table 6.** Adhesion and antifriction parameters ( $L_{c2}$ —load at which peeling of the coating areas from the substrate occurs and  $L_{c3}$ —critical load at which the indenter penetrates into the metal) of the coatings on the Mg-Mn-Ce system alloy samples [134].

Sample No.	Coating Type	$L_{c2}$ (N)	$L_{c3}$ (N)	Number of Cycles
1	PEO	$8.4 \pm 0.5$	$13.8 \pm 0.2$	2560
2	PEO + PVDF ( $\times 1$ )	$12.2 \pm 0.4$	$14.2 \pm 0.3$	2540
3	PEO + PVDF ( $\times 2$ )	$17.1 \pm 0.5$	$18.8 \pm 0.6$	64,826
4	PEO + PVDF ( $\times 3$ )	$18.2 \pm 0.2$	$18.8 \pm 0.3$	68,252

The results of electrochemical studies (Table 7) also show significant advantages of PVDF coating on PEO top layer. Even a single PVDF treatment reduces the current density by 2 orders of magnitude compared to a simple PEO coating.

**Table 7.** Comparison of electrochemical parameters ( $E_{\text{corr}}$ —free corrosion potential;  $i_{\text{corr}}$ —free corrosion currents;  $|Z|_{f=0.01}$ —alternating current polarization resistance) of the Mg-Mn-Ce system alloy samples with different coatings [134].

Cover Type	$E_{\text{corr}}$ (V)	$i_{\text{corr}}$ ( $\text{A}\cdot\text{cm}^{-2}$ )	$R_{\text{loss}}$ ( $\text{Om}\cdot\text{cm}^2$ )	$ Z _{f=0.01}$ ( $\text{Om}\cdot\text{cm}^2$ )
without cover	−1.56	$3.3 \times 10^{-5}$	$6.8 \times 10^2$	$7.2 \times 10^2$
PEO coating	−1.53	$1.4 \times 10^{-6}$	$6.7 \times 10^4$	$7.6 \times 10^4$
PEO + 1 layer PVDF	−1.41	$9.7 \times 10^{-8}$	$2.7 \times 10^5$	$3.5 \times 10^5$
PEO + 2 layers PVDF	−1.42	$6.1 \times 10^{-8}$	$4.6 \times 10^5$	$1.1 \times 10^6$
PEO + 3 layers PVDF	−1.31	$6.0 \times 10^{-9}$	$5.3 \times 10^6$	$2.8 \times 10^6$

Thus, the PVDF coating applied over the PEO coating gives good corrosion and anti-friction properties and can be used on various products.

Gnedenkov et al. [113] have produced multifunctional corrosion-resistant and bioactive coatings made of hydroxyapatite  $\text{Ca}_{10}(\text{PO}_4)_6(\text{OH})_2$  and magnesium oxide MgO, on Mg-Mn-Ce (Mg-2Mn-0.25Ce) alloy by PEO in an electrolyte containing calcium glycerophosphate and sodium fluoride. The PEO porous layers were post-treated using superdispersed PTFE powder, which penetrated into the porous hydroxyapatite layer. This, caused a considerable reduction of the magnesium alloy corrosion rate (>4 orders of magnitude). The coatings have a complex porous morphology which is favourable for osteoblast adhesion, simultaneously, reducing the corrosion rate of the magnesium alloy. This allows

the coating to be applied for biodegradable Mg implants. Moreover, sealing of the porous part of the coating by PTFE powder improves greatly the anticorrosion properties of Mg implants in physiological solution. Additional prospects of using organic and inorganic nanosized materials in the process of the formation of surface multifunctional composite protective layers obtained using plasma electrolytic oxidation on metals and alloys are discussed in the paper of Minaev et al. [135].

Dou et al. [136] prepared a bioactive micro-arc oxidation/chitosan (MAO/CS) composite coating on Mg-Zn-Ca (Mg-1.75Zn-0.56Ca) alloy for orthopaedic applications. The chitosan (CS) is a natural cationic polymer deriving from the natural occurring chitin through N-deacetylation. The polysaccharide CS has been approved for human clinical use due to its favourable biocompatibility, biodegradability and antibacterial activity. The MAO/CS composite coatings have been successfully produced on the Mg-Zn-Ca alloy via the dipping method, without pores, and with a smooth and defect-free surface. The MAO/CS coatings retained a low degradation rate and the solution pH value at a moderate level ( $\leq 7.5$ ) during the immersion test. The corrosion resistance and cell proliferation were greatly enhanced by the composite coating. Furthermore, *in vitro* immersion test suggests that it is bioactive and could promote cell proliferation and differentiation. Thus, it is expected that MAO/CS composite coating is a promising substitute for biomedical bone implants.

## 7. Physical Vapour Deposition

Physical vapour deposition (PVD) is a widely used technique for the fabrication of thin films and surface coatings. PVD has been applied at an industrial scale and combined with different methods to produce coatings with superior properties. Recent developments in nanoscience have made this technique more and more useful for the fabrication of layers with desired microstructure and properties. Recently, many PVD coating methods and their applications even in the field of cemented carbide tools have been significantly developed. However, only a few attempts for the production of Mg PVD coatings exhibit promising results, as described in scientific literature.

Several PVD coatings, metal and ceramic, single layers or multilayer systems, have been investigated to protect Mg alloys [137–140]. PVD technique is a feasible method for preparing protective metal coatings on magnesium alloy and can be an alternative to electrochemical methods. Both aluminium and titanium show good corrosion resistance in aggressive environments [141], moreover, Al galvanic compatibility with magnesium, although not ideal, is better than that of most other engineering metals [142]. A comparative study on the corrosion behaviour of Al, Ti, Zr and Hf metallic coatings deposited on AZ91D magnesium alloys was reported by Zhang et al. [143]. They found that the Hf-coated Mg alloy exhibits a superior anti-corrosion property after the SST, with only a few corrosion sites. The low difference in potential with the Mg alloy, the fine corrosion resistance and the good adhesion contributed to the superior anti-corrosion performance of the Hf coating.

No industrial PVD coatings are available that meet the requirements for corrosion protection of the magnesium alloys due to the risk of severe galvanic corrosion between substrate and coating. Hoche et al. have investigated TiMgN, TiMgYN and TiMgGdN coatings on AZ31 [144]. Coatings were fabricated by DC and HiPIMS (high-power impulse magnetron sputtering), and Gd was found to improve the corrosion resistance, probably thanks to the formation of a dense and stable oxide film able to prevent galvanic corrosion between coating and substrate. As expected, the HiPIMS coatings showed both improved corrosion and mechanical resistance.

In [145] the corrosion behaviour of an AZ91 alloy uncoated and coated with AlN-Al-AlN-Al-AlN and AlN-TiN multilayers fabricated by DC magnetron sputtering was investigated in a 0.6 M NaCl solution. Results showed that PVD coatings deposited on AZ91 increased the corrosion resistance of the alloy, and AlN + AlN + AlN coating increased the corrosion resistance much more than AlN + TiN coating. However, it was observed

that, in the coating layers, small structural defects like pores, pinholes and cracks could get the lower ability of protection from corrosion.

A research group from Poland published several works [146–148], where were reported successful implementations of hybrid coatings of Mg alloys by producing of Mg-Al intermetallic layer with a subsequential protective nitrides-PVD coating [146] and nano multilayer of AlN-CrN-TiN composite coating [147]. In Figure 10 is represented a common approach of the multilayer hybrid structure.

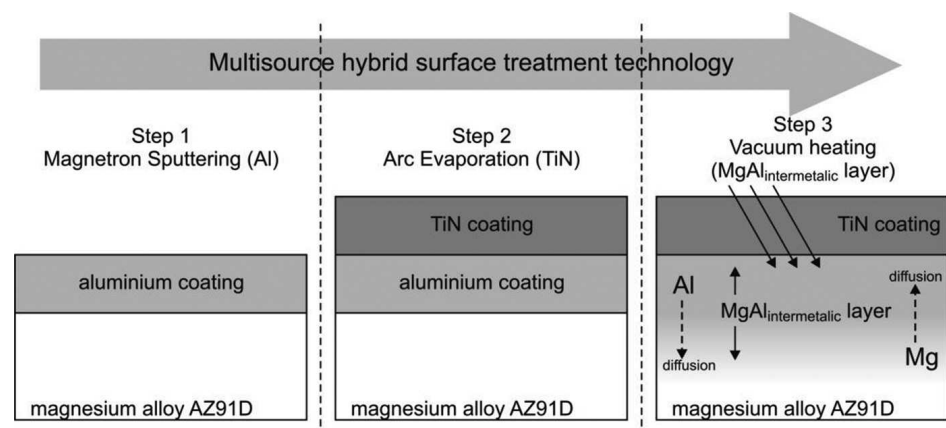


**Figure 10.** The scheme of a multisource hybrid surface treatment technology for the deposition of Mg-Al<sub>intermetallic</sub>/TiN composite layer. Reproduced from [146] with permission from Polish Academy of Sciences.

#### *Influence of the Surface Preparation before PVD Coating*

Appropriate surface preparation and/or surface activation are found necessary before the PVD deposition to improve coatings performances [57]. As an example, in [149] the authors developed a new method of plasma anodisation to ensure acceptable corrosion resistance to magnesium die-cast AZ91D alloy. Instead of a conventional anodization process using an aqueous electrolyte, an oxygen plasma was used, allowing anodising and PVD-coating in one process.

## 8. Laser Processes

### 8.1. Laser Cladding Method

In laser cladding (LC) a thick layer (generally thicker than 500  $\mu\text{m}$ ) of a protective material with a composition chemically different from the substrate material is bonded/fused on the surface of the substrate [150]. The scheme of LC process is shown in Figure 11. This method is characterized by the rapid release of laser energy in the near-surface region at extremely high temperatures, high heating and cooling rates (100~1000 K/s), which allows the deposition of a protective coating with nanocrystalline and even amorphous structure in the cladding layer on the substrate surface [151–153]. The process involves laser melting of the material to be clad on the substrate without significant dilution from the substrate, and because cladding material composition may differ from the base material, it becomes possible to select the composition of the protective coating with alloying elements that are not subject to corrosion, improving therefore corrosion and wearing behaviour of the magnesium alloys. In addition, the coating shows strong metallurgical bonding with substrate with a shallow heat affected zone, and the rapid heating and cooling rates ensure a fine and uniform microstructure. Most of the study reported in the literature deals with cladding of heterogeneous coatings based on Al-base alloys and Al-base metal-matrix composites. Al-base coatings could enhance the corrosion resistance giving at the same time good bonding properties to the interface. A review of recent developments of laser cladding on magnesium alloys was recently reported by Liu et al. [154]. In [155] a recent study on laser cladding and properties of AZ63-Er alloy for automobile engine was reported by Bu et al.

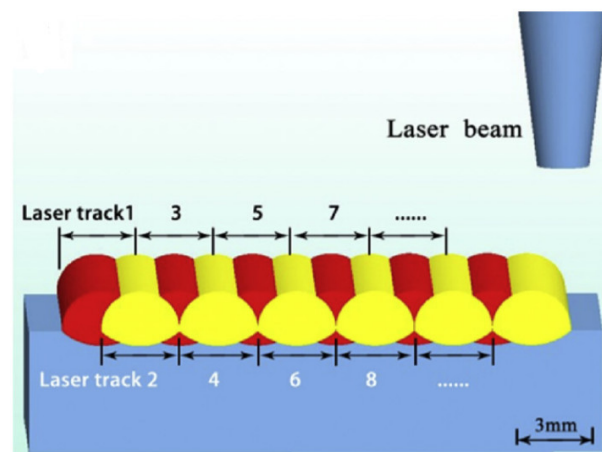


**Figure 11.** Laser cladding method scheme. Reproduced from [154] with permission from Elsevier.

The microstructure and the corrosion behaviour of a ZE41 alloy with laser surface cladding by Al-Si powder was studied in [126]. The chemical analysis of the clad layer showed Al-Mg system matrix with the precipitation of  $Mg_2Si$  dendrites. In the beginning, there is a dissolution of  $Mg_2Si$  particles acting as an anode, and then there is the initial stage of pitting corrosion in the resulting raster places. The pH level in the depth of the pitting decreases, and on the surface, on the contrary, increases. The acidic nature of the reaction promotes the formation of  $SiO_2$ . As a result, the potentials of the Al and  $Mg_{17}Al_{12}$  phases in the NaCl solution become close and the potential for the formation of corrosion and both metals become the same (Figure 12) [126].

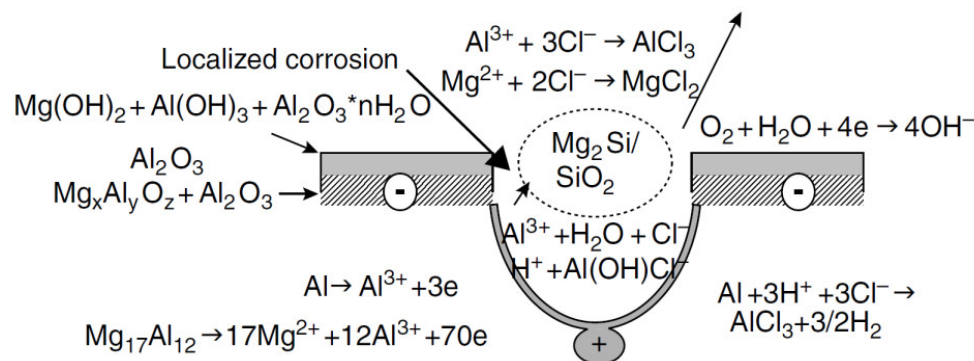


**Figure 12.** Schematic showing the localised corrosion mechanism of the intermetallic matrix in the presence of  $Mg_2Si$  particles. Reproduced from [126] with permission from Elsevier.

### 8.2. Protective Coating Using Powder or Filler Material

Laser surface alloying (LSA) is a similar process to LC but using high energy density. While LC is an incremental technique to produce coatings, LSA is a non-decremental technique which results in the formation of superficial technological layers [156]. In LSA, the chosen alloying elements are added to the melt pool to modify the surface composition of the base material. The alloying element can be introduced in two different ways, i.e., direct injection or preplaced coating [150]. LSA method makes it possible to develop a corrosion-resistant coating and apply it to the base material, thereby obtaining good corrosion protection regardless of the initial properties of the material. Laser alloying of the surface is effective for increasing the corrosion resistance of magnesium and its alloys. The correct choice of alloying elements providing good adhesion between the coating and the substrate, with a close melting point, is essential to provide a defect-free alloy zone

with improved corrosion resistance. The principle of laser surface alloying [156] in case of a pre-placed powder is shown in Figure 13.

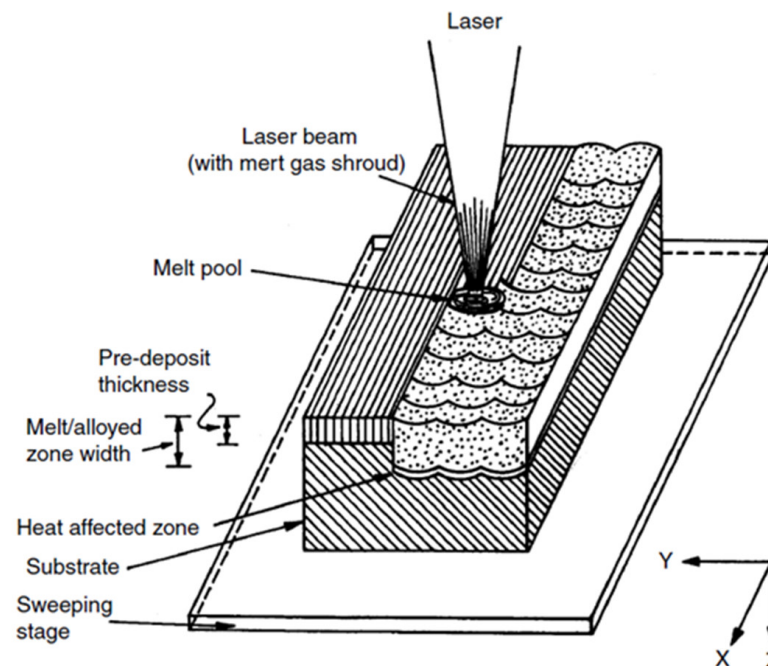


**Figure 13.** Schematic of laser surface alloying process using a pre-placed powder. Reproduced from [43] with permissions from Elsevier.

It is important to understand that cladding can be performed both with another magnesium alloy, for example, the Mg-Zr system, which has higher corrosion resistance, or with an alloy that does not have magnesium in its composition. Below is an example of modification of the surface layer of the MEZ alloy (Mg-RE-Zn-Zr, where RE stands for rare earths) Mg-2.5%RE-0.5%Zn [157] by Al-Mn system coatings (Figure 14) [158].

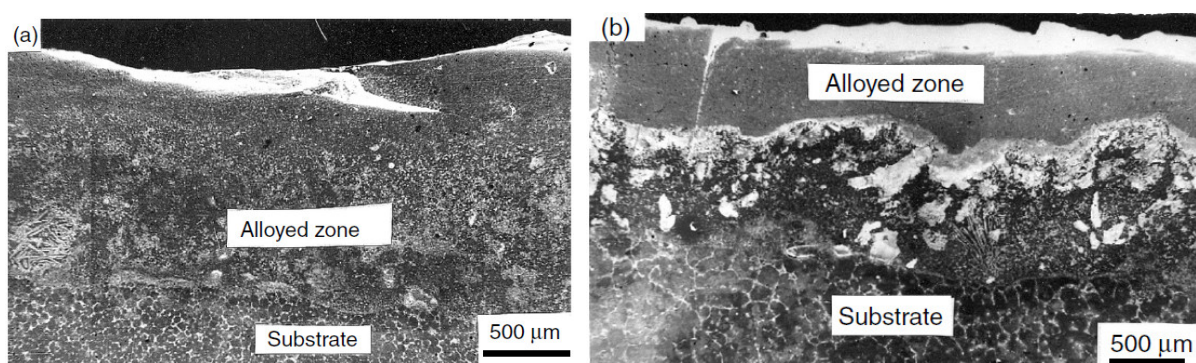


**Figure 14.** Scanning electron micrograph of the cross-section laser alloyed MEX with (a) 76Al + 24Mn and (b) 45Al + 55Mn lased with a power of laser with power of 2.5 kW, a scan speed of 200 mm/min and powder feed rate of 20 mg·s<sup>-1</sup>. Reproduced from [158] with permission from Elsevier.

The addition of an Mn-Al alloy gives fairly good corrosion properties. The paper shows the research results obtained using a CO<sub>2</sub> laser. The surface was processed at a beam power of 2.5 kW, at a speed of 200 mm·min<sup>-1</sup>, and the powder was fed at a speed of 20 mg·s<sup>-1</sup>. The surfacing was carried out in an argon atmosphere. The cross section of the coated specimen shown in Figure 14 is mainly composed of Al + Mn and Al + Mg intermetallics. The maximum content of Al and Mn is on the surface and decreases as it

approaches the substrate. The resulting uniform structure contributes to good corrosion protection, but it is important to understand that such a structure can be obtained only in a narrow range of laser operation parameters, which requires precise tuning [158].

Table 8 shows the results of corrosion tests of the initial material, the material with a laser-treated surface and the material with the deposition of an alloy of the Al-Mn system in 3.5% NaCl solution carried out within 72 h [158].

**Table 8.** Summary of the parameters (OCP—open circuit potential;  $E_{\text{corr}}$ —free corrosion potential;  $i_{\text{corr}}$ —free corrosion current) defining the corrosion behaviour of as-received and laser surface alloyed MEZ under different conditions in a 3.5% NaCl solution [158].

Sample	OCP (mV)	$E_{\text{corr}}$ (mV)	$i_{\text{corr}}$ (mA)	Corrosion Rate (mpy)
MEZ (as-received)	−1528	−1531	1.714	1521.3
MEZ (laser-remelted)	−1185	−1181	0.875	777.3
Laser surface alloyed with 76Al + 24Mn	−1445	−1448	0.286	254.5
Laser surface alloyed with 45Al + 55Mn	−1441	−1437	0.230	204.32

### 8.3. High-Energy Laser Treatment of the Metal Surface: Laser Shock Peening Method

A promising method of surface treatment with a laser beam is primarily due to the ability to effectively transfer a certain amount of thermal energy to a given depth of the alloy surface. Method of surface treatment with a laser beam like laser shock peening (LSP) process consists of fast surface treatment with a laser [43,159,160]. As a result, a shock wave is generated due to an increase in the volume of the plasma arc on the surface. Due to this, a change in the microstructure of the surface layer occurs. To increase the surface treatment effect (increase the cooling rate of the melted layer), the treatment is carried out through a layer of water, and the surface is painted with dark paint for better energy absorption [159]. When exposed to LSP, the chemical composition of the base metal remains the same; there is no possibility of adding alloying components to increase the corrosion resistance. Also, after processing, the surface of the product remains rough, which makes the appearance of the final product not very attractive. However, this disadvantage manifests itself on the positive side when using magnesium alloys as biocompatible implants. A rough surface is best suited for the fusion of living tissue with an implant [161].

In the case of applying protective coatings by anodizing, preliminary surface preparation plays an important role [133]. Thus, the surface formed after LSP treatment can serve as a good basis for applying coatings by anodizing [125].

A common disadvantage of both methods is that the coverage is carried out only in the line of sight, that is, in places where direct laser penetration can be achieved. Machining parts of complex shape with areas inaccessible to direct laser hits is not suitable for these surface treatment methods. Also, the speed of laser surface treatment is currently not high and is more suitable for processing small products or local surface treatment.

The principal scheme of the LSP is shown in Figure 15. Laser action is characterized by instant heating and extremely fast cooling, which allows the formation of a structure on the surface of the product with increased hardness, while not affecting the structure and properties of the base metal [43]. The laser shock peening method has several advantages, for example, it is environmentally friendly in contrast to the method of electroplating, which also requires accurate surface preparation. In the case of comparison with CCCs, the surface treated with LSP retains its properties at elevated temperatures, while most CCCs do not withstand temperatures above 65 °C [150,162,163].

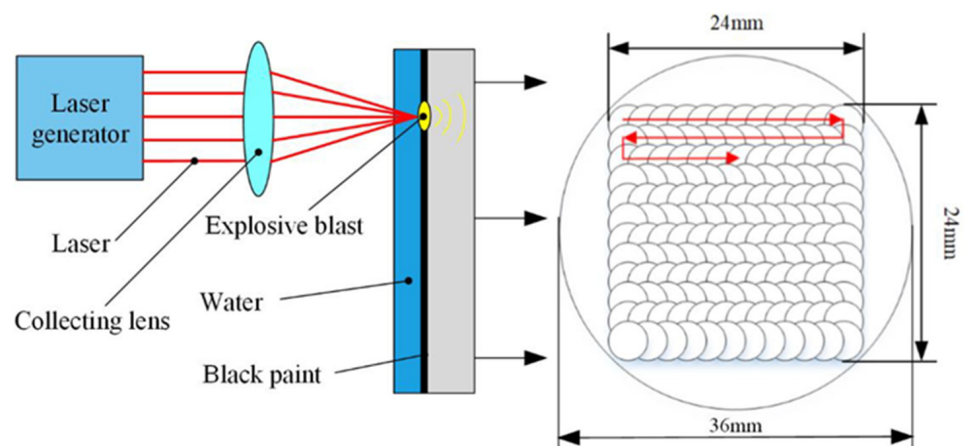


**Figure 15.** Schematic diagram of laser shock peening and the pattern of laser impact path. Adapted from [159].

During processing, a strong refinement of the grain structure occurs (Figure 16), which has a positive effect on the resistance to stress corrosion cracking, probably due to a decrease in electrochemical corrosion, as well as an increase in wear resistance. In addition, an improvement in characteristics such as material hardness and fatigue strength can be observed.

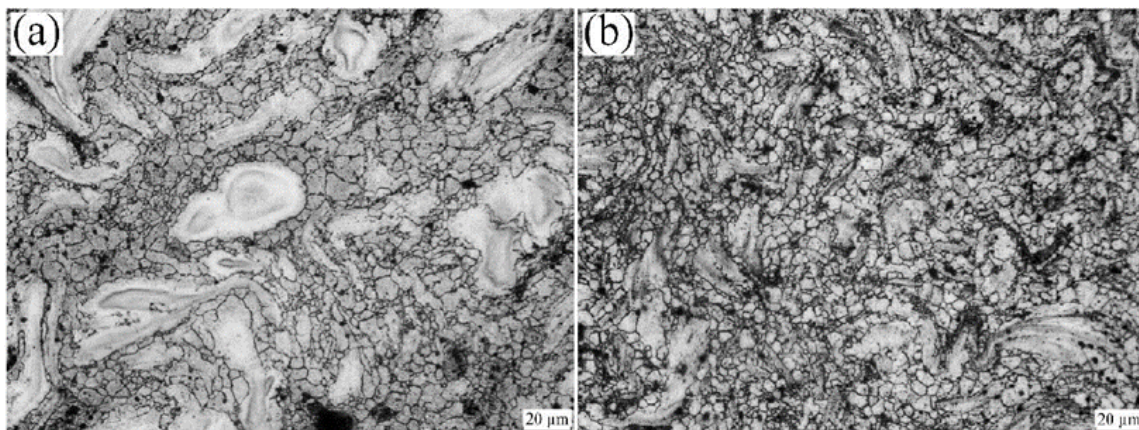


**Figure 16.** The surface microstructure of ZK60 before and after laser impact: (a) untreated; (b)  $1.19 \text{ GW} \cdot \text{cm}^{-2}$  [159].

After the surface treatment with the LSP method, the weight loss in corrosion tests of alloy ZK60 in simulated body fluid (SBF) solution was reduced by 52%, and the overall corrosion resistance increased by 20% [159].

As already mentioned, a distinctive point is the possible presence of surface roughness after laser treatment. This phenomenon can be evaluated as negative because it can spoil the appearance of the product, however, in the case of using a magnesium alloy to create biodegradable implants, this parameter, on the contrary, promotes better cell adhesion and growth of inert tissue. Chemical analysis showed an increase in the proportion of calcium and fluorine content (Figure 17), which also demonstrates the applicability of ZK60 alloy processed by the LSP method in the production of biodegradable implants [159].

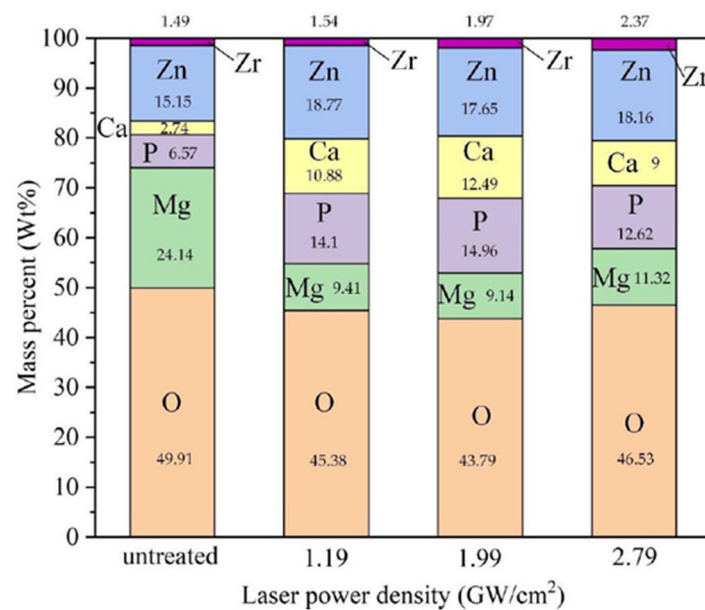


Figure 17. Elemental mass percentages of EDS spectral results. Adapted from [159].

#### 8.4. Coating Types

In work [153], the Laser Cladding method was used to apply coatings consisting of a mixture of Al-Cu-Zn powders with different atomic ratios (at%):  $\text{Al}_{80}\text{Cu}_{15}\text{Zn}_5$ ,  $\text{Al}_{85}\text{Cu}_{10}\text{Zn}_5$ , and  $\text{Al}_{90}\text{Cu}_5\text{Zn}_5$  (Figure 18). The advantage of choosing a coating comprising of a mixture of Al, Zn, Cu powders is a prospect for obtaining a protective surface with an amorphous structure. LC is an efficient method of producing amorphous aluminium-based coatings due to the aforementioned extremely high cooling rates. Earlier, it was proved that an amorphous structure exists in thin films of Al-Zn-Cu obtained by DC magnetron sputtering [153,161].

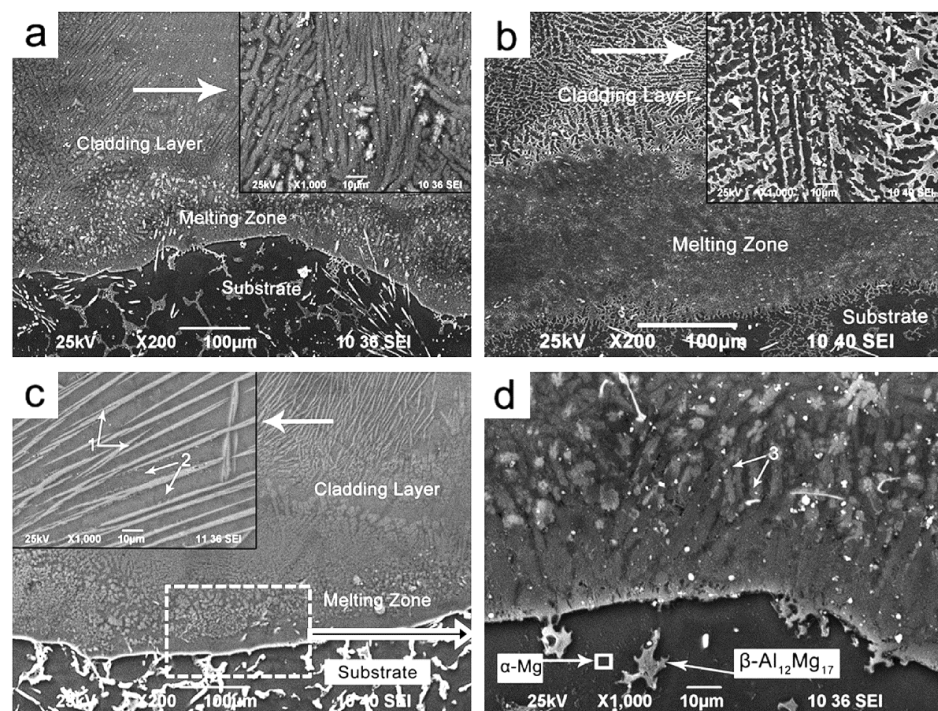
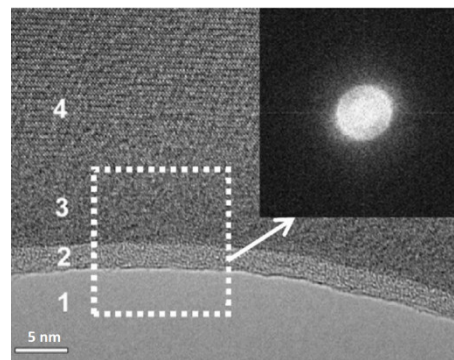


Figure 18. Substrate and deposited layer structures (a)  $\text{Al}_{80}\text{Cu}_{15}\text{Zn}_5$ , (b)  $\text{Al}_{90}\text{Cu}_5\text{Zn}_5$ , (c,d)  $\text{Al}_{85}\text{Cu}_{10}\text{Zn}_5$ . Reproduced from [153] with permission from Elsevier.

In the melting zone, a columnar structure with a crystal size of the order of 70–120  $\mu\text{m}$  was found, which indicates that the substrate has a stable metallurgical bond with the deposited layer. In the layer with the composition  $\text{Al}_{80}\text{Cu}_{15}\text{Zn}_5$ , the structure is close to nanocrystalline or amorphous. X-ray structural analysis of the structure characterized in the form of needles with the composition  $\text{Al}_{85}\text{Cu}_{10}\text{Zn}_5$  showed the presence of the  $\text{Mg}_{32}\text{Al}_{47}\text{Cu}_7$  phase. Selected area electron diffraction (SAED) images of the  $\text{Al}_{80}\text{Cu}_{15}\text{Zn}_5$  coating (Figure 19) indicate that the structure in this layer is mainly amorphous [153].



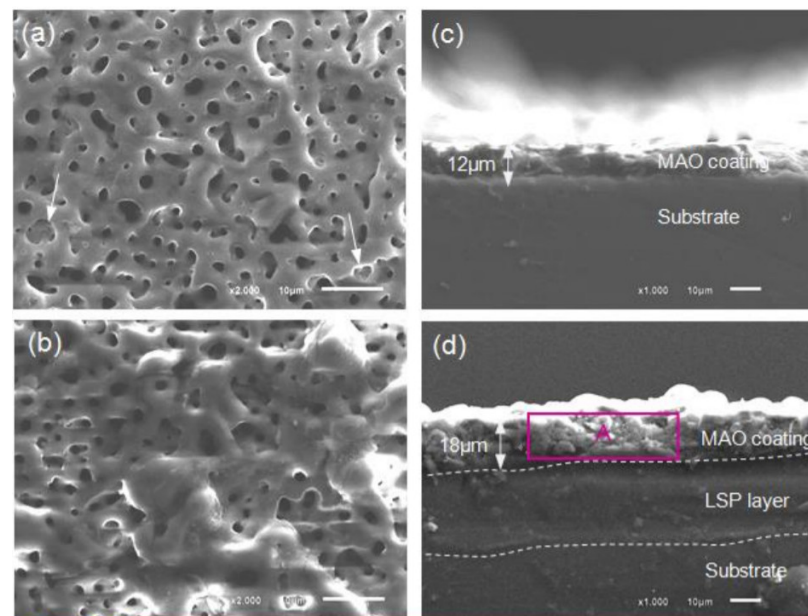
**Figure 19.** Bright-field TEM image and corresponding SAED pattern for the amorphous phases. Reproduced from [134] with permission from Elsevier.

Thus, it can be assumed that the LC method allows obtaining an amorphous structure on the surface of the substrate of the AZ80 alloy, which should increase the corrosion resistance and maintain the mechanical properties of the coating upon short-term deformation of the substrate. It is important to note the absence of visible defects, given that the height of the protective coating is about 1 mm.

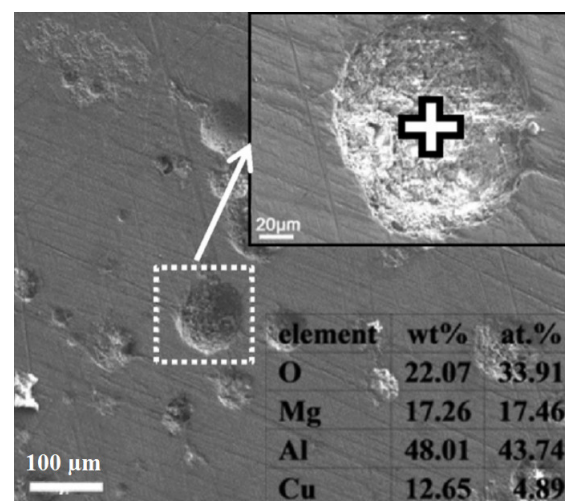
A completely different structure (Figure 20) is shown on samples coated with the MAO and LSP/MAO methods. First, it should be noted that the thickness of the protective layer is 12–18  $\mu\text{m}$ , and the surface also has a porous structure, although the pore size is only  $\sim 5 \mu\text{m}$ . This can affect the accelerated development of corrosion. Perhaps, in the case of using the device as a biocompatible implant, such micropores could become centres of interaction between the implant and living tissue, but a similar structure was also observed in works where the main goal was not related to the development of biodegradable medical implants [125].

Figure 20 clearly shows the LSP layer, which is about 20  $\mu\text{m}$ . The MAO coating bond is tighter to the LSP layer than to the untreated substrate surface. The MAO layer grown on the LSP treated surface is 18  $\mu\text{m}$  versus 12  $\mu\text{m}$  grown on the untreated surface. Thus, the LSP method allows increasing the protective properties at least by increasing the thickness of the protective layer.

However, compared to the LC method, the surface quality obtained by the MAO and LSP/MAO methods will be rather poor. Even after five wet-dry cycles using a 3.5% NaCl solution on the sample with the surface obtained by LC (Figure 21), fairly evenly distributed traces of surface damage are observed, indicating the development of pitting corrosion [153].



**Figure 20.** SEM images of surface morphology and cross-section of MAO sample (a,c) and LSP/MAO sample (b,d). Reproduced from [125] with permission from Elsevier.



**Figure 21.** Structure of substrate a and protective coating after exposure to 3.5% NaCl environment. Reproduced from [153] with permission from Elsevier.

Table 9 presents the electrochemical data obtained from the potentiodynamic polarization test on a AZ80 alloy and a AZ80 alloy coated with laser cladding after exposure to a 3.5% NaCl solution [153]. Table 10 reports the electrochemical data for an uncoated AZ80 alloy and the AZ80 alloy coated with MAO, LSP and LSP/MAO in a simulated body fluid environment [125].

**Table 9.** Electrochemical data ( $E_{\text{corr}}$ —free corrosion potential;  $i_{\text{corr}}$ —free corrosion current) obtained from potentiodynamic polarisation test for uncoated AZ80 and AZ80 coated with Al<sub>85</sub>Cu<sub>10</sub>Zn<sub>5</sub> cladding layer [153].

Sample	$E_{\text{corr}}$ (mV)	$i_{\text{corr}}$ (A/cm <sup>2</sup> )
Uncoated AZ80	−1524	$8.34 \times 10^{-6}$
AZ80 coated with LC	−1247	$7.62 \times 10^{-4}$

**Table 10.** Electrochemical data ( $E_{\text{corr}}$ —free corrosion potential;  $i_{\text{corr}}$ —free corrosion current) obtained from potentiodynamic polarisation test for uncoated AZ80 and coated with different techniques [125].

Sample	$E_{\text{corr}}$ (mV)	$i_{\text{corr}}$ (A/cm <sup>2</sup> )
Uncoated AZ80	$-1482 \pm 10$	$1.54 \times 10^{-5} \pm 0.34 \times 10^{-5}$
AZ80 coated with LSP	$-1517 \pm 20$	$2.13 \times 10^{-6} \pm 0.29 \times 10^{-6}$
AZ80 coated with MAO	$-1431 \pm 20$	$7.35 \times 10^{-7} \pm 0.41 \times 10^{-7}$
AZ80 coated with LSP/MAO	$-1347 \pm 15$	$2.73 \times 10^{-7} \pm 0.35 \times 10^{-7}$

From Tables 9 and 10, it can be seen that the greatest increase in corrosion potential is observed when using the LC technique, for an amount of 277 mV. When using the LSP/MAO method, the  $E_{\text{corr}}$  difference is 135 mV. Processing only by the MAO method gives an ennoblement to the material, in terms of  $E_{\text{corr}}$ , equal to 51 mV concerning bare AZ80 alloy; the LSP method itself did not give any increase of  $E_{\text{corr}}$ ; on the contrary, the  $E_{\text{corr}}$  increased by 35 mV, although the measurement error should be taken into account. Tables 9 and 10 show comparisons of the corrosion properties of various coatings in NaCl and SBF solutions that were applied to AZ80 alloy. Base of SBF solution is NaCl compound [125]. Of course, the concentration of NaCl in the SBF solution will be different, as there are other compounds in the solution, which can also indirectly affect the research results. But in the absence of studies with the same initial data, this comparison allows us to assess the prospects of using the methods.

#### 8.5. Summary of Laser Processes

Material analysis research has shown that the use of the LC method in comparison with LSP and LSP/MAO shows significantly higher corrosion resistance results. The LC method allows more flexibility in the selection of surface protection components. The use of a laser makes it possible to obtain a protective layer of a given thickness with a good affinity for the base material. The possibility of obtaining a coating with an amorphous structure suggests that the use of this method is promising for products experiencing short-term loads as a result of which there is a temporary change in geometry while maintaining the primary protective properties, and also significantly reduces the value of corrosion resistance.

The use of the LSP technique is justified if it is necessary to prepare the surface for coating by anodizing, in particular MAO. The coating applied to the substrate pretreated by the LSP method makes it possible to obtain a more dense bond of the coating with the substrate material, increase the thickness of the coating, and also more effectively reduce the corrosion potential of the surface.

### 9. Surface Preparation before Anti-Corrosion Treatment

Often when conducting research, as well as in commercial production, insufficient attention is paid to the process of preparing the surface of the material for anti-corrosion treatment, although a thorough pre-treatment may allow for maximum adhesion and to get the best anti-corrosion performance. An example of processing order is shown in Figure 22.

**Figure 22.** Standard initial steps of a process chain of handling magnesium surfaces (conversion coating in this example).

Untimely removal of contaminating particles of emulsion, oil, etc., as well as the too long time between treatment and coating, entails the penetration of corrosion activators under the surface of the protective coating, which entails conditions favourable for the

development of corrosion and accelerated destruction of the product. Surface treatments can be divided into two stages: mechanical and chemical. When machining, it is very important to choose the processing method so as not to damage the surface.

Chemical etching can be as neutral surfactants, alkali, acid, organic solvents using a degreaser. The choice of reagent for chemical etching is dictated by the goal that the etching wants to achieve. In some cases, either mechanical or chemical cleaning is sufficient. Figure 23 shows iron inclusions on the Mg surface, after various methods of surface treatment [145].

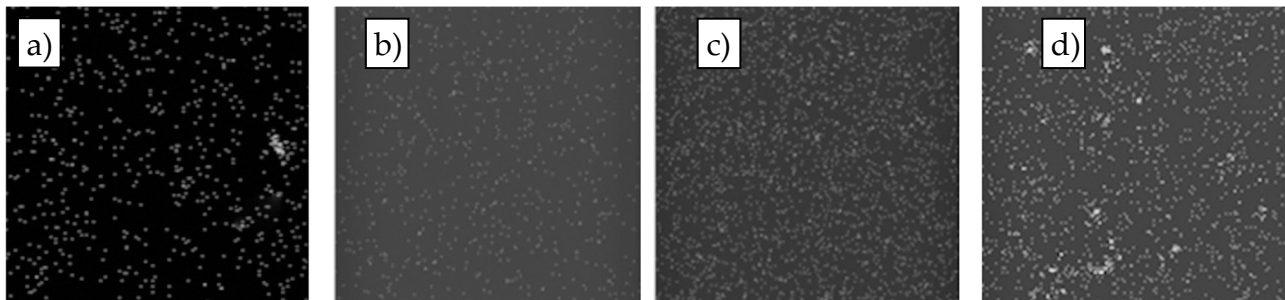


**Figure 23.** Fe mapping on AZ31 sample surfaces: (a) as-received, (b) abraded, (c) acid cleaned, (d) and blasted. The white particles shown in the mapping are Fe-containing impurities. Reproduced from [164] with permission from Elsevier.

The work [133] presents the results of surface preparation of the Mg-Al-Zn-Mn alloy system before applying a PEO coating. Figure 24 shows the structure of the PEO coating formed in the areas with the  $Mg_{17}Al_{12}$  (Figure 24a,b) and  $Al_xMn_y$  (Figure 24c) phases.

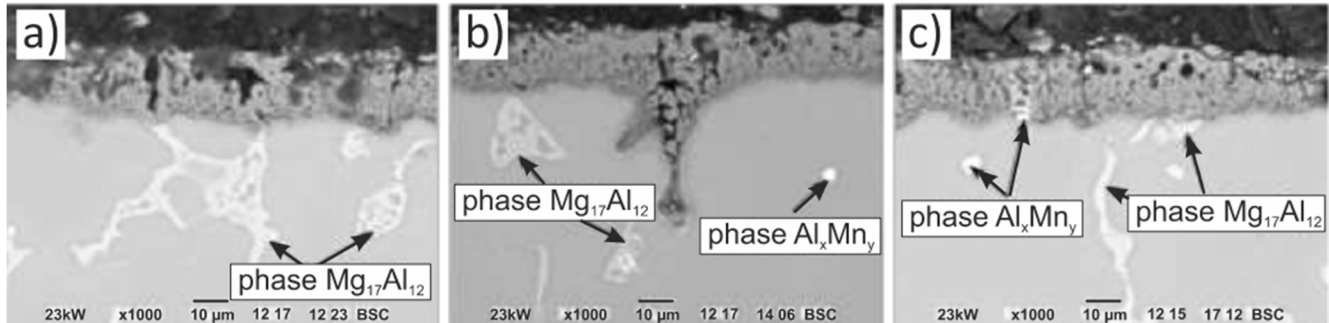


**Figure 24.** Cross-section of ML5 alloy with PEO coating: (a) section of a PEO coating formed on the  $Mg_{17}Al_{12}$  phase, which was initially on the surface of the alloy; (b) section of PEO-coating formed at the site of the  $Mg_{17}Al_{12}$  phase, deep in the magnesium alloy; (c) area of the PEO coating with a minimum number of through defects formed on the  $Al_8Mn_2$  phase initially located on the alloy surface. Adapted from [133].

It follows from the figure that in the area where the coating was formed in the places where the  $Mg_{17}Al_{12}$  and  $Al_xMn_y$  phases were absent, there are no surface defects. In the areas where the phases were formed, large defects and through pores are observed. When a PEO layer is formed, a dense barrier oxide layer of various thicknesses is formed on the sample surface. In the areas where the  $Mg_{17}Al_{12}$  and  $Al_xMn_y$  phases are present, the thickness and electrical resistance of the barrier layer are lower, and as a result, the corrosion protection is worse. Figure 25 shows the result of applying a PEO layer after etching with various solutions.

The result presented in Figure 25a shows the minimum number of defects and pores even in the presence of aluminium-containing phases. PEO coating formed on a surface prepared with an alkaline solution has a greater number of defects, but they are much smaller than the sample which was not subjected to surface treatment.

Based on the data obtained, it can be concluded that preliminary etching allows the surface to be prepared for the optimal formation of the PEO layer. It is the quality of surface preparation that determines the stability of the formation of a protective PEO layer. The choice of surface preparation solution will depend on the chemical composition of the alloy.

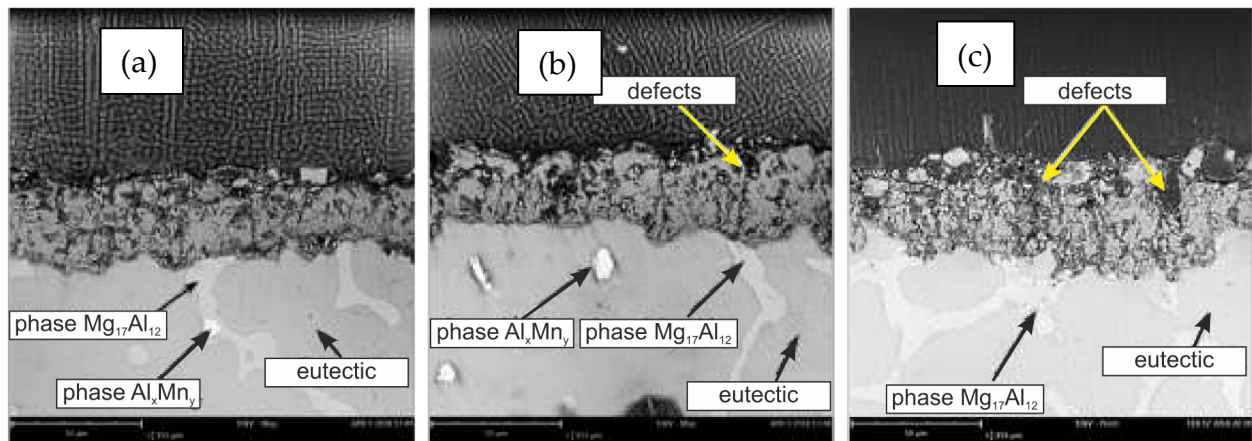


**Figure 25.** Cross-sections of samples with PEO-coating during etching in solutions of HF (a) and NaOH (b); (c)—without etching. Adapted from [133].

## 10. Conclusions

Currently, there are new effective methods of protecting magnesium alloys from corrosion. Unlike traditional protection by electrochemical machining and deposition of coatings, modern methods allow not only to protect the alloy against corrosion but also to improve its surface mechanical and tribological properties thanks to the application of coatings and surface modification layer structures.

Correct surface preparation can significantly increase the effect of anti-corrosion treatments and has a positive effect on the resource of the products used. Thus, the chemical treatment allows several times to increase the protective properties of the alloy surface due to the possibility of creating a defect-free protective layer.

Sequential complex processing of various types of protective coatings allows obtaining superior anti-corrosion properties as compared to those obtained if single coatings were applied separately, allowing expanding the application of magnesium alloys in various industrial fields.

**Author Contributions:** Conceptualization, M.L., V.Z. and E.P.; formal analysis, M.L., D.R., P.P. and G.R.; investigation, M.L.G., B.O.P., M.L., D.R., P.P., V.Z.; resources, M.L., V.Z. and E.P.; data curation, B.O.P., M.L., V.Z. and P.P.; writing—original draft preparation M.L.G., B.O.P., M.L., D.R., V.Z. and P.P.; writing—review and editing, M.L.G., P.P., D.R., M.L., B.O.P., V.Z., G.R., E.P. and M.L.; visualization, D.R., B.O.P., G.R.; supervision, E.P. and M.L.; project administration, E.P.; funding acquisition, E.P. and M.L. All authors have read and agreed to the published version of the manuscript.

**Funding:** The part of research conducted by Pavel Predko, Eleonora Pole, and Marks Lisnanskis was funded by the European Regional Development Fund within the scope of the project “Innovative and efficient coating development for magnesium components”, agreement No. 1.1.1.1/19/A/148.



INVESTING IN YOUR FUTURE

**Data Availability Statement:** The data presented in this study are available on request from the authors.

**Acknowledgments:** Useful discussions with Tiziano Bellezze, from UNIPM, are gratefully acknowledged.

**Conflicts of Interest:** The authors declare no conflict of interest.

## References

1. Maier, P.; Clausius, B.; Wicke, J.; Hort, N. Characterization of an Extruded Mg-Dy-Nd Alloy during Stress Corrosion with C-Ring Tests. *Metals* **2020**, *10*, 584. [[CrossRef](#)]
2. Xie, Q.; Ma, A.; Jiang, J.; Cheng, Z.; Song, D.; Yuan, Y.; Liu, H. Stress Corrosion Cracking Behavior of Fine-Grained AZ61 Magnesium Alloys Processed by Equal-Channel Angular Pressing. *Metals* **2017**, *7*, 343. [[CrossRef](#)]
3. Gupta, N.; Paramsothy, M. Metal- and Polymer-Matrix Composites: Functional Lightweight Materials for High-Performance Structures. *JOM* **2014**, *66*, 862–865. [[CrossRef](#)]
4. Manakari, V.; Parande, G.; Doddamani, M.; Gaitonde, V.N.; Siddhalingeswar, I.G.; Kishore Shunmugasamy, V.C.; Gupta, N. Dry sliding wear of epoxy/cenosphere syntactic foams. *Tribol. Int.* **2015**, *92*, 425–438. [[CrossRef](#)]
5. Jayavardhan, M.L.; Bharath Kumar, B.R.; Doddamani, M.; Singh, A.K.; Zeltmann, S.E.; Gupta, N. Development of glass microballoon/HDPE syntactic foams by compression molding. *Compos. Part B Eng.* **2017**, *130*, 119–131. [[CrossRef](#)]
6. Luong, D.; Lehmus, D.; Gupta, N.; Weise, J.; Bayoumi, M. Structure and Compressive Properties of Invar-Cenosphere Syntactic Foams. *Materials* **2016**, *9*, 115. [[CrossRef](#)]
7. Peroni, L.; Scapin, M.; Avalle, M.; Weise, J.; Lehmus, D.; Baumeister, J.; Busse, M. Syntactic Iron Foams—On Deformation Mechanisms and Strain-Rate Dependence of Compressive Properties. *Adv. Eng. Mater.* **2012**, *14*, 909–918. [[CrossRef](#)]
8. Peroni, L.; Scapin, M.; Lehmus, D.; Baumeister, J.; Busse, M.; Avalle, M.; Weise, J. High Strain Rate Tensile and Compressive Testing and Performance of Mesoporous Invar (FeNi36) Matrix Syntactic Foams Produced by Feedstock Extrusion. *Adv. Eng. Mater.* **2017**, *19*, 1600474. [[CrossRef](#)]
9. Weise, J.; Lehmus, D.; Baumeister, J.; Kun, R.; Bayoumi, M.; Busse, M. Production and Properties of 316L Stainless Steel Cellular Materials and Syntactic Foams. *Steel Res. Int.* **2014**, *85*, 486–497. [[CrossRef](#)]
10. Weise, J.; Salk, N.; Jehring, U.; Baumeister, J.; Lehmus, D.; Bayoumi, M.A. Influence of powder size on production parameters and properties of syntactic invar foams produced by means of metal powder injection moulding. *Adv. Eng. Mater.* **2013**, *15*, 118–122. [[CrossRef](#)]
11. Luong, D.D.; Shunmugasamy, V.C.; Gupta, N.; Lehmus, D.; Weise, J.; Baumeister, J. Quasi-static and high strain rates compressive response of iron and Invar matrix syntactic foams. *Mater. Des.* **2015**, *66*, 516–531. [[CrossRef](#)]
12. Manakari, V.; Parande, G.; Doddamani, M.; Gupta, M. Evaluation of wear resistance of magnesium/glass microballoon syntactic foams for engineering/biomedical applications. *Ceram. Int.* **2019**, *45*, 9302–9305. [[CrossRef](#)]
13. Qureshi, W.; Kannan, S.; Vincent, S.; Eddine, N.N.; Muhammed, A.; Gupta, M.; Karthikeyan, R.; Badari, V. Influence of silica nanospheres on corrosion behavior of magnesium matrix syntactic foam. In Proceedings of the International Conference on Recent Advances in Materials & Manufacturing Technologies, Dubai, United Arab Emirates, 28–29 November 2017; Institute of Physics Publishing: Bristol, UK, 2018; Volume 346.
14. Manakari, V.; Parande, G.; Gupta, M. Effects of hollow fly-ash particles on the properties of magnesium matrix syntactic foams: A review. *Mater. Perform. Charact.* **2016**, *5*, 116–131. [[CrossRef](#)]
15. Shishkin, A.; Mironov, V.; Zemchenkov, V.; Antonov, M.; Hussainova, I. Hybrid Syntactic Foams of Metal—Fly Ash Cenosphere—Clay. *Key Eng. Mater.* **2016**, *674*, 35–40. [[CrossRef](#)]
16. Shishkin, A.; Mironov, V.; Zemchenkov, V.; Hussainova, I. Metal Powder/Fly Ash Cenosphere/Modified Clay, Composite. In Proceedings of the EURO PM2014 Congress: PM Functional Materials, Salzburg, Austria, 21–24 September 2014; p. 117821.
17. Shishkin, A.; Hussainova, I.; Kozlov, V.; Lisnanskis, M.; Leroy, P.; Lehmus, D. Metal-Coated Cenospheres Obtained via Magnetron Sputter Coating: A New Precursor for Syntactic Foams. *JOM* **2018**, *70*, 1319–1325. [[CrossRef](#)]
18. Tatarinov, A.; Shishkin, A.; Mironov, V. Correlation between ultrasound velocity, density and strength in metal-ceramic composites with added hollow spheres. *IOP Conf. Ser. Mater. Sci. Eng.* **2019**, *660*, 012040. [[CrossRef](#)]
19. Rugele, K.; Lehmus, D.; Hussainova, I.; Peculevica, J.; Lisnanskis, M.; Shishkin, A. Effect of Fly-Ash Cenospheres on Properties of Clay-Ceramic Syntactic Foams. *Materials* **2017**, *10*, 828. [[CrossRef](#)]
20. Shishkin, A.; Laksa, A.; Shidlovska, V.; Timermane, Z.; Aguedal, H.; Mironov, V.; Ozolins, J. Illite Clay Ceramic Hollow Sphere—Obtaining and Properties. *Key Eng. Mater.* **2016**, *721*, 316–321. [[CrossRef](#)]
21. Huo, W.; Zhang, X.; Chen, Y.; Lu, Y.; Liu, J.; Yan, S.; Wu, J.-M.; Yang, J. Novel mullite ceramic foams with high porosity and strength using only fly ash hollow spheres as raw material. *J. Eur. Ceram. Soc.* **2017**, *38*, 1–8. [[CrossRef](#)]
22. Ren, S.; Tao, X.; Xu, X.; Guo, A.; Liu, J.; Fan, J.; Ge, J.; Fang, D.; Liang, J. Preparation and characteristic of the fly ash cenospheres/mullite composite for high-temperature application. *Fuel* **2018**, *233*, 336–345. [[CrossRef](#)]
23. Shishkin, A.; Bumanis, G.; Irtiseva, K.; Ozolins, J.; Korjaks, A. Clay Ceramic Hollow Sphere—Cement Syntactic Foam Composite for Building Applications. *Key Eng. Mater.* **2019**, *800*, 228–234. [[CrossRef](#)]
24. Baronins, J.; Setina, J.; Sahmenko, G.; Lagzdina, S.; Shishkin, A. Pore Distribution and Water Uptake in a Cenosphere-Cement Paste Composite Material. *IOP Conf. Ser. Mater. Sci. Eng.* **2015**, *96*, 012011. [[CrossRef](#)]
25. Irtiseva, K.; Lapkovskis, V.; Mironov, V.; Ozolins, J.; Thakur, V.K.; Goel, G.; Baronins, J.; Shishkin, A. Towards Next-Generation Sustainable Composites Made of Recycled Rubber, Cenospheres, and Biobinder. *Polymers* **2021**, *13*, 574. [[CrossRef](#)]

26. Campbell, F.C. (Ed.) *Lightweight Materials: Understanding the Basics*; EngineeringPro Collection; ASM International: Materials Park, OH, USA, 2012; ISBN 9781615039906.
27. Benefits | Clean Sky. Available online: <https://www.cleansky.eu/benefits> (accessed on 21 March 2021).
28. NACE Rev. 2. *Manufacturing Statistics—Data Extracted in March 2020*; Eurostat: Luxembourg, 2020.
29. Hamilton, B.A.; McLean, VA, USA. Aluminum Cost Profiles. Unpublished Report, 2013; Analyses Are Based on Costs Reported by Hale, W.R., The Global Light Metals Sector Outlook: A Primary Aluminum Perspective, Industrial Insight. November 2000; 26–30.
30. Wulandari, W.; Brooks, G.A.; Rhamdhani, M.A.; Monaghan, B.J. Magnesium: Current and Alternative Production Routes. In Proceedings of the Australasian Conference on Chemical Engineering, Adelaide, Australia, 26–29 September 2010; pp. 1–11.
31. Nie, J.-F. Physical Metallurgy of Light Alloys. In *Physical Metallurgy*; Elsevier: Amsterdam, The Netherlands, 2014; pp. 2009–2156.
32. Ehrenberger, S. *Life Cycle Assessment of Magnesium Components in Vehicle Construction*; German Aerospace Centre: Stuttgart, Germany, 2013.
33. European Commission. *Study on the EU's List of Critical Raw Materials (2020), Factsheets on Critical Raw Materials*; European Commission: Brussels, Belgium, 2020.
34. Grant, P. *Chemistry Input into the Manufacturing of Novel Materials and Future Trends in Food Manufacturing*; Government Office for Science: London, UK, 2013.
35. Annamalai, S.; Periyakgoundar, S.; Gunasekaran, S. Magnesium alloys: A review of applications. *Mater. Tehmol.* **2019**, *53*, 881–890. [[CrossRef](#)]
36. Easton, M.; Qian Song, W.; Abbott, T. A comparison of the deformation of magnesium alloys with aluminium and steel in tension, bending and buckling. *Mater. Des.* **2006**, *27*, 935–946. [[CrossRef](#)]
37. Pegguleryuz, M.; Labelle, P.; Argo, D. *Magnesium Die Casting Alloy AJ62x with Superior Creep Resistance, Ductility and Die Castability*; SAE International: Warrendale, PA, USA, 2003.
38. Mordike, B.L.; Ebert, T. Magnesium Properties—Applications—Potential. *Mater. Sci. Eng. A* **2001**, *302*, 37–45. [[CrossRef](#)]
39. Matmatch. Available online: <https://matmatch.com/learn/material/magnesium-alloys> (accessed on 10 July 2021).
40. Makar, G.L.; Kruger, J. Corrosion Studies of Rapidly Solidified Magnesium Alloys. *J. Electrochem. Soc.* **1990**, *137*, 414–421. [[CrossRef](#)]
41. Takeno, N. *Atlas of Eh-pH Diagrams. Intercomparison of Thermodynamic Databases*; National Institute of Advanced Industrial Science and Technology: Tokyo, Japan, 2005.
42. Song, G.L. *Corrosion Electrochemistry of Magnesium (Mg) and Its Alloys*; Woodhead Publishing Limited: Cambridge, UK, 2011; ISBN 9781845697082.
43. Dutta Majumdar, J.; Manna, I. Laser treatment to improve the corrosion resistance of magnesium (Mg) alloys. In *Corrosion Prevention of Magnesium Alloys*; Elsevier: Amsterdam, The Netherlands, 2013; pp. 133–162.
44. Bratsch, S.G. Standard Electrode Potentials and Temperature Coefficients in Water at 298.15 K. *J. Phys. Chem. Ref. Data* **1989**, *18*, 1–21. [[CrossRef](#)]
45. Альтман, М.Б.; Антипова, А.П.; Тимонина, М.А.; Чухров, М.В. *Магниеиые сплаиы, 1-я часть: Металлоиедение магниия и его сплавов. Области применения*; Металлургия: Москва, Россия, 1978. (In Russian)
46. Luo, A.A. Magnesium casting technology for structural applications. *J. Magnes. Alloys* **2013**, *1*, 2–22. [[CrossRef](#)]
47. Cashion, S.; Ricketts, N.; Hayes, P. The mechanism of protection of molten magnesium by cover gas mixtures containing sulphur hexafluoride. *J. Light Met.* **2002**, *2*, 43–47. [[CrossRef](#)]
48. Baronins, J.; Podgursky, V.; Antonov, M.; Bereznev, S.; Hussainova, I. Electrochemical Behaviour of TiCN and TiAlN Gradient Coatings Prepared by Lateral Rotating Cathode Arc PVD Technology. *Key Eng. Mater.* **2016**, *721*, 414–418. [[CrossRef](#)]
49. Radha, R.; Sreekanth, D. Insight of magnesium alloys and composites for orthopedic implant applications—A review. *J. Magnes. Alloys* **2017**, *5*, 286–312. [[CrossRef](#)]
50. Zhao, L.; Cui, C.; Wang, Q.; Bu, S. Growth characteristics and corrosion resistance of micro-arc oxidation coating on pure magnesium for biomedical applications. *Corros. Sci.* **2010**, *52*, 2228–2234. [[CrossRef](#)]
51. Wang, J.; Pang, X.; Jahed, H. Surface protection of Mg alloys in automotive applications: A review. *AIMS Mater. Sci.* **2019**, *6*, 567–600. [[CrossRef](#)]
52. Grilli, M.L.; Valerini, D.; Piticescu, R.R.; Bellezze, T.; Yilmaz, M.; Rinaldi, A.; Cuesta-López, S.; Rizzo, A. Possible alternatives to critical elements in coatings for extreme applications. *IOP Conf. Ser. Mater. Sci. Eng.* **2018**, *329*, 012005. [[CrossRef](#)]
53. Baronins, J.; Antonov, M.; Bereznev, S.; Raadik, T.; Hussainova, I. Raman Spectroscopy for Reliability Assessment of Multilayered AlCrN Coating in Tribo-Corrosive Conditions. *Coatings* **2018**, *8*, 229. [[CrossRef](#)]
54. Antonov, M.; Afshari, H.; Baronins, J.; Adoberg, E.; Raadik, T.; Hussainova, I. The effect of temperature and sliding speed on friction and wear of Si<sub>3</sub>N<sub>4</sub>, Al<sub>2</sub>O<sub>3</sub>, and ZrO<sub>2</sub> balls tested against AlCrN PVD coating. *Tribol. Int.* **2018**, *118*, 500–514. [[CrossRef](#)]
55. Baronins, J.; Antonov, M.; Bereznev, S.; Raadik, T.; Hussainova, I. Raman Spectroscopy of Multilayered AlCrN Coating under High Temperature Sliding/Oxidation. *Key Eng. Mater.* **2019**, *799*, 9–14. [[CrossRef](#)]
56. Wang, Y.; Normand, B.; Liao, H.; Zhao, G.; Mary, N.; Tang, J. SiCp/Al5056 Composite Coatings Applied to A Magnesium Substrate by Cold Gas Dynamic Spray Method for Corrosion Protection. *Coatings* **2020**, *10*, 325. [[CrossRef](#)]
57. Liu, F. Effect of Pretreatment and Annealing on Aluminum Coating Prepared by Physical Vapor Deposition on AZ91D Magnesium Alloys. *Int. J. Electrochem. Sci.* **2016**, *11*, 5655–5668. [[CrossRef](#)]

58. Magnesium Alloys Market Size and Forecast. Available online: <https://www.verifiedmarketresearch.com/product/magnesium-alloys-market/> (accessed on 16 July 2021).
59. Global Magnesium Alloys Market—Industry Trends and Forecast to 2027. Available online: <https://www.databridgemarketresearch.com/reports/global-magnesium-alloys-market> (accessed on 16 July 2021).
60. European Commission. *Communication from the Commission to the European Parliament, the Council, the European Economic and Social Committee and the Committee of the Regions ‘Tackling the Challenges in Commodity Markets and on Raw Materials’*; COM/2011/0025 Final; European Commission: Brussels, Belgium, 2011.
61. European Commission. *Communication from the Commission to the European Parliament, the Council, the European Economic and Social Committee and the Committee of the Regions: On the Review of the List of Critical Raw Materials for the EU and the Implementation of the Raw Material*; European Commission: Brussels, Belgium, 2017.
62. European Commission. *Communication from the Commission to the European Parliament, the Council, the European Economic and Social Committee and the Committee of the Regions on the 2017 List of Critical Raw Materials for the EU*; European Commission: Brussels, Belgium, 2017.
63. European Commission. *Communication from the Commission to the European Parliament, the Council, the European Economic and Social Committee and the Committee of the Regions ‘Critical Raw Materials Resilience: Charting a Path towards greater Security and Sustainability’*; COM/2020/474 Final; European Commission: Brussels, Belgium, 2020.
64. Department of the Interior of the US Final List of Critical Minerals 2018. *Fed. Regist.* **2018**, *83*, 23295–23296.
65. U. S. Geological Survey. *Mineral Commodity Summaries 2020: U.S. Geological Survey*; U.S. Geological Survey: Reston, VA, USA, 2020.
66. European Commission. *Study on the EU’s list of Critical Raw Materials (2020)—Final Report*; European Commission: Brussels, Belgium, 2020.
67. Grilli, M.L.; Valerini, D.; Slobozeanu, A.E.; Postolnyi, B.O.; Balos, S.; Rizzo, A.; Piticescu, R.-R. Critical raw materials saving by protective coatings under extreme conditions: A review of last trends in alloys and coatings for aerospace engine applications. *Materials* **2021**, *14*, 1052. [[CrossRef](#)]
68. European Commission. Development of Innovative Nanocomposite Coatings for Magnesium Castings Protection. Available online: <https://cordis.europa.eu/project/id/G1RD-CT-2002-00692/results> (accessed on 21 April 2021).
69. Corrosion and Inspection of General Aviation Aircraft, CAP 1570, Published by the Civil Aviation Authority, 2017 Civil Aviation Authority Aviation House Gatwick Airport South West Sussex RH6 0YR. Available online: [https://publicapps.caa.co.uk/docs/33/CAP1570\\_Corrosion.pdf](https://publicapps.caa.co.uk/docs/33/CAP1570_Corrosion.pdf) (accessed on 21 April 2021).
70. Song, J.; She, J.; Chen, D.; Pan, F. Latest research advances on magnesium and magnesium alloys worldwide. *J. Magnes. Alloys* **2020**, *8*, 1–41. [[CrossRef](#)]
71. Ramalingam, V.V.; Ramasamy, P.; Das Kovukkal, M.; Myilsamy, G. Research and Development in Magnesium Alloys for Industrial and Biomedical Applications: A Review. *Met. Mater. Int.* **2020**, *26*, 409–430. [[CrossRef](#)]
72. Liu, H.; Cao, F.; Song, G.-L.; Zheng, D.; Shi, Z.; Dargusch, M.S.; Atrens, A. Review of the atmospheric corrosion of magnesium alloys. *J. Mater. Sci. Technol.* **2019**, *35*, 2003–2016. [[CrossRef](#)]
73. Zhang, D.; Peng, F.; Liu, X. Protection of magnesium alloys: From physical barrier coating to smart self-healing coating. *J. Alloys Compd.* **2021**, *853*, 157010. [[CrossRef](#)]
74. Song, G.L.; Atrens, A. Corrosion Mechanisms of Magnesium Alloys. *Adv. Eng. Mater.* **1999**, *1*, 11–33. [[CrossRef](#)]
75. Witte, F.; Fischer, J.; Nellesen, J.; Crostack, H.-A.; Kaese, V.; Pisch, A.; Beckmann, F.; Windhagen, H. In vitro and in vivo corrosion measurements of magnesium alloys. *Biomaterials* **2006**, *27*, 1013–1018. [[CrossRef](#)]
76. Song, G. Recent Progress in Corrosion and Protection of Magnesium Alloys. *Adv. Eng. Mater.* **2005**, *7*, 563–586. [[CrossRef](#)]
77. Esmaily, M.; Svensson, J.E.; Fajardo, S.; Birbilis, N.; Frankel, G.S.; Virtanen, S.; Arrabal, R.; Thomas, S.; Johansson, L.G. Fundamentals and advances in magnesium alloy corrosion. *Prog. Mater. Sci.* **2017**, *89*, 92–193. [[CrossRef](#)]
78. European Commission, Multiscale Analysis of Fatigue in Mg Alloys. Available online: <https://cordis.europa.eu/project/id/795658> (accessed on 21 April 2021).
79. Perrin, M.X. Synergistic Corrosion Protection for Magnesium Alloys—SYNPROMAG. Available online: <https://anr.fr/Project-ANR-18-ASTR-0016> (accessed on 21 April 2021).
80. Aluminium and Magnesium Alloys Green Innovative Coatings. Available online: <https://cordis.europa.eu/project/id/755515> (accessed on 21 April 2021).
81. Controlling the Degradation of Magnesium Alloys for Biomedical Applications Using Innovative Smart Coatings. Available online: <https://www.ua.pt/en/projetos-id/129> (accessed on 21 April 2021).
82. European Commission. Industrial Pilot Plant for Semisolid Process Route with Eco-Compatible Feedstock Materials. Available online: [https://ec.europa.eu/environment/life/project/Projects/index.cfm?fuseaction=search.dspPage&n\\_proj\\_id=5766](https://ec.europa.eu/environment/life/project/Projects/index.cfm?fuseaction=search.dspPage&n_proj_id=5766) (accessed on 21 April 2021).
83. European Commission. Localized Corrosion Studies for Magnesium Implant Devices. Available online: <https://cordis.europa.eu/project/id/703566> (accessed on 21 April 2021).
84. European Commission. Development of Smart Nano and Microcapsulated Sensing Coatings for Improving of Material Durability/Performance. Available online: <https://cordis.europa.eu/project/id/645662> (accessed on 21 April 2021).
85. European Commission. Multi-Functional Metallic Surfaces via Active Layered Double Hydroxide Treatments. Available online: <https://cordis.europa.eu/project/id/645676> (accessed on 21 April 2021).

86. European Commission. New Recovery Processes to Produce Rare Earth-Magnesium Alloys of High Performance and Low Cost. Available online: <https://cordis.europa.eu/project/id/680629> (accessed on 21 April 2021).
87. Perrin, M.X. Magnésium Résistant Corrosion Peinture Optimisée Liant Organique. Available online: <https://mapiem.univ-tln.fr/MAGnesium-Resistant-CORrosion-Peinture-Optimisee-Liant-Organique.html> (accessed on 21 April 2021).
88. European Commission. Eco-Friendly Corrosion Protecting Coating of Aluminium and Magnesium Alloys. Available online: <https://www.aidic.it/cet/14/41/029.pdf> (accessed on 21 April 2021).
89. European Commission. Development and Implementation of Conductive Coating for Magnesium Sheets in A/C. Available online: <https://cordis.europa.eu/project/id/297173> (accessed on 21 April 2021).
90. European Commission. Advanced Environmentally Friendly Chemical Surface Treatments for Cast Magnesium Helicopter Transmission Alloys Preservation. Available online: <https://cordis.europa.eu/project/id/307659> (accessed on 21 April 2021).
91. European Commission. Corrosion Protective Coating on Light Alloys by Micro-Arc Oxidation. Available online: <https://cordis.europa.eu/project/id/270589> (accessed on 21 April 2021).
92. European Commission. Tailored Biodegradable Magnesium Implant Materials. Available online: <https://cordis.europa.eu/project/id/289163> (accessed on 21 April 2021).
93. R&D Projects: Fault-Tolerant Anticorrosion Coatings for Magnesium Alloys. Available online: [https://www.fct.pt/apoios/projetos/consulta/vglobal\\_projecto?idProjecto=112831&idElemConcurso=3618](https://www.fct.pt/apoios/projetos/consulta/vglobal_projecto?idProjecto=112831&idElemConcurso=3618) (accessed on 21 April 2021).
94. European Commission. Environmentally Acceptable Pretreatment System for Painting Multi Metals. Available online: <https://cordis.europa.eu/project/id/262473> (accessed on 21 April 2021).
95. European Commission. Multi-Level Protection of Materials for Vehicles by “Smart” Nanocontainers. Available online: <https://cordis.europa.eu/project/id/214261> (accessed on 21 April 2021).
96. Development of Steel Fastener Nano-Ceramic Coatings for Corrosion Protection of Magnesium Parts. Available online: <https://www.energy.gov/eere/vehicles/downloads/development-steel-fastener-nano-ceramic-coatings-corrosion-protection> (accessed on 21 April 2021).
97. Wu, C.Y.; Zhang, J. State-of-art on corrosion and protection of magnesium alloys based on patent literatures. *Trans. Nonferr. Met. Soc. China (Engl. Ed.)* **2011**, *21*, 892–902. [CrossRef]
98. Liu, X.; Yue, Z.; Romeo, T.; Weber, J.; Scheuermann, T.; Moulton, S.; Wallace, G. Biofunctionalized anti-corrosive silane coatings for magnesium alloys. *Acta Biomater.* **2013**, *9*, 8671–8677. [CrossRef] [PubMed]
99. Talha, M.; Ma, Y.; Xu, M.; Wang, Q.; Lin, Y.; Kong, X. Recent Advancements in Corrosion Protection of Magnesium Alloys by Silane-Based Sol-Gel Coatings. *Ind. Eng. Chem. Res.* **2020**, *59*, 19840–19857. [CrossRef]
100. Chen, X.B.; Birbilis, N.; Abbott, T.B. Review of Corrosion-Resistant Conversion Coatings for Magnesium and Its Alloys. *Corrosion* **2011**, *67*, 035005-1–035005-16. [CrossRef]
101. Marlaud, T.; Malki, B.; Henon, C.; Deschamps, A.; Baroux, B. Relationship between alloy composition, microstructure and exfoliation corrosion in Al–Zn–Mg–Cu alloys. *Corros. Sci.* **2011**, *53*, 3139–3149. [CrossRef]
102. Hu, R.G.; Zhang, S.; Bu, J.F.; Lin, C.J.; Song, G.L. Recent progress in corrosion protection of magnesium alloys by organic coatings. *Prog. Org. Coat.* **2012**, *73*, 129–141. [CrossRef]
103. Yao, W.; Liang, W.; Huang, G.; Jiang, B.; Atrens, A.; Pan, F. Superhydrophobic coatings for corrosion protection of magnesium alloys. *J. Mater. Sci. Technol.* **2020**, *52*, 100–118. [CrossRef]
104. Gray, J.E.; Luan, B. Protective coatings on magnesium and its alloys—A critical review. *J. Alloys Compd.* **2002**, *336*, 88–113. [CrossRef]
105. Zhang, J.; Wu, C. Corrosion and Protection of Magnesium Alloys—A Review of the Patent Literature. *Recent Patents Corros. Sci.* **2010**, *2*, 55–68. [CrossRef]
106. Hu, H.; Nie, X.; Ma, Y. Corrosion and Surface Treatment of Magnesium Alloys. In *Magnesium Alloys—Properties in Solid and Liquid States*; InTech: London, UK, 2014; Volume I, p. 13.
107. Lamaka, S.V.; Knörschild, G.; Snihirova, D.V.; Taryba, M.G.; Zheludkevich, M.L.; Ferreira, M.G.S. Complex anticorrosion coating for ZK30 magnesium alloy. *Electrochim. Acta* **2009**, *55*, 131–141. [CrossRef]
108. Tong, L.B.; Zhang, J.B.; Xu, C.; Wang, X.; Song, S.Y.; Jiang, Z.H.; Kamado, S.; Cheng, L.R.; Zhang, H.J. Enhanced corrosion and wear resistances by graphene oxide coating on the surface of Mg–Zn–Ca alloy. *Carbon N. Y.* **2016**, *109*, 340–351. [CrossRef]
109. Sang, J.; Kang, Z.X.; Li, Y.Y. Corrosion resistance of Mg–Mn–Ce magnesium alloy modified by polymer plating. *Trans. Nonferr. Met. Soc. China (Engl. Ed.)* **2008**, *18*, s374–s379. [CrossRef]
110. Fang, H.; Wang, C.; Zhou, S.; Li, G.; Tian, Y.; Suga, T. Exploration of the enhanced performances for silk fibroin/sodium al-ginate composite coatings on biodegradable Mg–Zn–Ca alloy. *J. Magnes. Alloys* **2020**. [CrossRef]
111. Kartsonakis, I.A.; Balaskas, A.C.; Koumoulos, E.P.; Charitidis, C.A.; Kordas, G. Evaluation of corrosion resistance of magnesium alloy ZK10 coated with hybrid organic-inorganic film including containers. *Corros. Sci.* **2012**, *65*, 481–493. [CrossRef]
112. Liu, Q.; Kang, Z. Preparation and micro-tribological property of hydrophobic organic films on the surface of Mg–Mn–Ce magnesium alloy. *Prog. Org. Coat.* **2015**, *84*, 42–49. [CrossRef]
113. Gnedenkov, S.V.; Sinebryukhov, S.L.; Zavidnaya, A.G.; Egorin, V.S.; Puz, A.V.; Mashtalyar, D.V.; Sergienko, V.I.; Yerokhin, A.L.; Matthews, A. Composite hydroxyapatite-PTFE coatings on Mg–Mn–Ce alloy for resorbable implant applications via a plasma electrolytic oxidation-based route. *J. Taiwan Inst. Chem. Eng.* **2014**, *45*, 3104–3109. [CrossRef]

114. Gadow, R.; Gammel, F.J.; Lehnert, F.; Scherer, D.; Skar, J.I. Coating System for Magnesium Diecastings in Class A Surface Quality. In *Magnesium Alloys and Their Applications*; Wiley-VCH Verlag GmbH & Co. KGaA: Weinheim, Germany, 2006; pp. 492–498. ISBN 3527302824.
115. Kaseem, M.; Hussain, T.; Rehman, Z.U.; Ko, Y.G. Stabilization of AZ31 Mg alloy in sea water via dual incorporation of MgO and WO<sub>3</sub> during micro-arc oxidation. *J. Alloys Compd.* **2021**, *853*, 157036. [[CrossRef](#)]
116. Kaseem, M.; Hussain, T.; Zeeshan, U.R.; Yang, H.W.; Dikici, B.; Ko, Y.G. Fabrication of functionalized coating with a unique flowery-flake structure for an effective corrosion performance and catalytic degradation. *Chem. Eng. J.* **2021**, *420*, 129737. [[CrossRef](#)]
117. Синебрюхов, С.Л.; Сидорова, М.В.; Егоркин, В.С.; Недозоров, П.М.; Устинов, А.Ю.; Волкова, Е.Ф.; Гнеденков, С.В. Protective oxide coatings on magnesium alloys of the Mg-Mn-Ce, Mg-Zn-Zr, Mg-Al-Zn-Mn, Mg-Zn-Zr-Y and Mg-Zr-Nd systems (In Russian)—Защитные оксидные покрытия на магниевых сплавах систем Mg-Mn-Ce, Mg-Zn-Zr, Mg-Al-Zn-Mn, Mg-Zn-Zr-Y и Mg-Zr-Nd. *Физикохимия поверхности и защита материалов* **2012**, *48*, 23.
118. Gnedenkov, S.V.; Sinebryukhov, S.L.; Mashtalyar, D.V.; Nadaraia, K.V.; Gnedenkov, A.S.; Bouzник, V.M. Composite fluoropolymer coatings on the MA8 magnesium alloy surface. *Corros. Sci.* **2016**, *111*, 175–185. [[CrossRef](#)]
119. Dunleavy, C.S.; Golosnoy, I.O.; Curran, J.A.; Clyne, T.W. Characterisation of discharge events during plasma electrolytic oxidation. *Surf. Coat. Technol.* **2009**, *203*, 3410–3419. [[CrossRef](#)]
120. Duan, H.; Yan, C.; Wang, F. Effect of electrolyte additives on performance of plasma electrolytic oxidation films formed on magnesium alloy AZ91D. *Electrochim. Acta* **2007**, *52*, 3785–3793. [[CrossRef](#)]
121. Barati Darband, G.; Aliofkhaeaei, M.; Hamghalam, P.; Valizade, N. Plasma electrolytic oxidation of magnesium and its alloys: Mechanism, properties and applications. *J. Magnes. Alloys* **2017**, *5*, 74–132.
122. Sinebryukhov, S.L.; Sidorova, M.V.; Egorкин, V.S.; Nedozorov, P.M.; Ustinov, A.Y.; Gnedenkov, S.V. Anti-corrosion, anti-friction coatings on magnesium alloys for aviation (In Russian)—Антикоррозионные, антифрикционные покрытия на магниевых сплавах для авиации. *Bull. Far East. Branch Russ. Acad. Sci.* **2011**, *5*, 95–105.
123. Kossenko, A.; Zinigrad, M. Special Features of Oxide Layer Formation on Magnesium Alloys during Plasma Electrolytic Oxidation. *Glas. Phys. Chem.* **2018**, *44*, 62–70. [[CrossRef](#)]
124. Kossenko, A.; Zinigrad, M. A universal electrolyte for the plasma electrolytic oxidation of aluminum and magnesium alloys. *Mater. Des.* **2015**, *88*, 302–309. [[CrossRef](#)]
125. Xiong, Y.; Hu, Q.; Song, R.; Hu, X. LSP/MAO composite bio-coating on AZ80 magnesium alloy for biomedical application. *Mater. Sci. Eng. C* **2017**, *75*, 1299–1304. [[CrossRef](#)] [[PubMed](#)]
126. Volovitch, P.; Masse, J.E.; Fabre, A.; Barrallier, L.; Saikaly, W. Microstructure and corrosion resistance of magnesium alloy ZE41 with laser surface cladding by Al-Si powder. *Surf. Coat. Technol.* **2008**, *202*, 4901–4914.
127. Kozlov, I.A.; Karimov, S.A. Corrosion of magnesium alloys and modern methods of protection. *Aviat. Mater. Technol.* **2014**, 15–20. [[CrossRef](#)]
128. Жиликов, В.П.; Каримова, С.А.; Лешко, С.С.; Чесноков, Д.В. Investigation of the dynamics of corrosion of aluminum alloys when tested in a salt fog chamber (In Russian)—Исследование динамики коррозии алюминиевых сплавов при испытании в камере солевого тумана (Кст). *Авиационные Материалы и Технологии* **2014**, *4*, 18–22.
129. Каримова, С.А.; Павловская, Т.Г. Development of Corrosion Protection Methods for Structures Working in Space (In Russian)—Разработка Способов Защиты От Коррозии Конструкций, Работающих В Условиях Космос. *Авиационные материалы и технологии* **2013**, *S1*, 35–40.
130. Ribeiro, A.A.; Vaz, L.G.; Guastaldi, A.C.; Campos, J.S.C. Adhesion strength characterization of PVDF/HA coating on cp Ti surface modified by laser beam irradiation. *Appl. Surf. Sci.* **2012**, *258*, 10110–10114. [[CrossRef](#)]
131. Гнеденков, С.В.; Синебрюхов, С.Л.; Машталар, Д.В.; Надараиа, К.В.; Минаев, А.Н. Формирование защитных композиционных покрытий на магниевом сплаве с применением водной суспензии ультрадисперсного политетрафторэтилена (Formation of protective composite coatings on a magnesium alloy using an aqueous suspension of ultra-dispersed polytetrafluoroethylene in Russian). *Вестник Дальневосточного отделения Российской академии наук* **2016**, *6*, 77–82.
132. Song, G.-L.; Xu, Z. The surface, microstructure and corrosion of magnesium alloy AZ31 sheet. *Electrochim. Acta* **2010**, *55*, 4148–4161. [[CrossRef](#)]
133. Kozlov, I.A.; Vinogradov, S.S.; Uridiya, Z.P.; Duyunova, V.A.; Manchenko, V.A. Effect of preliminary etching of alloy ML5 before plasma electrolytic oxidation. *Proc. VIAM* **2018**, *9*, 32–42. [[CrossRef](#)]
134. Egorкин, V.; Vyalii, I.; Opra, D.; Sinebryukhov, S.; Gnedenkov, S. Electrochemical and Mechanical Properties of the PVDF/PEO-Coatings on Magnesium Alloy. *Solid State Phenom.* **2015**, *245*, 130–136. [[CrossRef](#)]
135. Minaev, A.N.; Gnedenkov, S.V.; Sinebryukhov, S.L.; Mashtalyar, D.V.; Sidorova, M.V.; Tsvetkov, Y.V.; Samokhin, A.V. Composite coatings formed by plasma electrolytic oxidation. *Prot. Met. Phys. Chem. Surfaces* **2011**, *47*, 840–849. [[CrossRef](#)]
136. Dou, J.; Wang, J.; Lu, Y.; Chen, C.; Yu, H.; Ma, R.L.W. Bioactive MAO/CS composite coatings on Mg-Zn-Ca alloy for orthopedic applications. *Prog. Org. Coat.* **2021**, *152*, 106112. [[CrossRef](#)]
137. Hoche, H.; Blawert, C.; Broszeit, E.; Berger, C. Galvanic corrosion properties of differently PVD-treated magnesium die cast alloy AZ91. *Surf. Coat. Technol.* **2005**, *193*, 223–229. [[CrossRef](#)]
138. Tański, T.; Labisz, K.; Lukaszowicz, K.; Śliwa, A.; Gołombek, K. Characterisation and properties of hybrid coatings deposited onto magnesium alloys. *Surf. Eng.* **2014**, *30*, 927–932. [[CrossRef](#)]

139. Navinšek, B.; Panjan, P.; Milošev, I. PVD coatings as an environmentally clean alternative to electroplating and electroless processes. *Surf. Coatings Technol.* **1999**, *116–119*, 476–487. [[CrossRef](#)]
140. Abela, S. Protective Coatings for Magnesium Alloys. In *Magnesium Alloys—Corrosion and Surface Treatments*; InTech: London, UK, 2011.
141. Wu, G. Fabrication of Al and Al/Ti coatings on magnesium alloy by sputtering. *Mater. Lett.* **2007**, *61*, 3815–3817. [[CrossRef](#)]
142. Liu, L. *Development of Novel Nanocomposite PVD Coatings to Improve Wear and Corrosion Resistance of Magnesium Alloys*; University of Sheffield: Sheffield, UK, 2017.
143. Zhang, D.; Wei, B.; Wu, Z.; Qi, Z.; Wang, Z. A comparative study on the corrosion behaviour of Al, Ti, Zr and Hf metallic coatings deposited on AZ91D magnesium alloys. *Surf. Coat. Technol.* **2016**, *303*, 94–102. [[CrossRef](#)]
144. Hoche, H.; Groß, S.; Oechsner, M. Development of new PVD coatings for magnesium alloys with improved corrosion properties. *Surf. Coat. Technol.* **2014**, *259*, 102–108. [[CrossRef](#)]
145. Altun, H.; Sen, S. The effect of PVD coatings on the corrosion behaviour of AZ91 magnesium alloy. *Mater. Des.* **2006**, *27*, 1174–1179. [[CrossRef](#)]
146. Smolik, J.; Mazurkiewicz, A.; Kacprzyńska-Gołacka, J.; Rydzewski, M. Composite layers tialintermetallic/PVD coating obtained by hybrid surface treatment technology on aluminium alloys. *Solid State Phenom.* **2015**, *237*, 34–40. [[CrossRef](#)]
147. Kacprzyńska-Gołacka, J.; Smolik, J.; Mazurkiewicz, A.; Bujak, J.; Garbacz, H.; Wieceński, P. The Influence of Microstructure of Nanomultilayer AlN-CrN-TiN Coatings on their Tribological Properties at Elevated Temperature. *Solid State Phenom.* **2015**, *237*, 27–33. [[CrossRef](#)]
148. Mazurkiewicz, A.; Smolik, J.; Pačko, D.; Kacprzyńska-Gołacka, J.; Garbacz, H.; Wieceński, P. The study on erosive and abrasive wear resistance of different multilayer coatings obtained on titanium alloy Ti6Al4V. *Solid State Phenom.* **2015**, *237*, 9–14. [[CrossRef](#)]
149. Hoche, H.; Scheerer, H.; Probst, D.; Broszeit, E.; Berger, C. Development of a plasma surface treatment for magnesium alloys to ensure sufficient wear and corrosion resistance. *Surf. Coat. Technol.* **2003**, *174–175*, 1018–1023. [[CrossRef](#)]
150. Singh, A.; Harimkar, S.P. Laser Surface Engineering of Magnesium Alloys: A Review. *JOM* **2012**, *64*, 716–733. [[CrossRef](#)]
151. Wang, C.; Jiang, B.; Liu, M.; Ge, Y. Corrosion characterization of micro-arc oxidization composite electrophoretic coating on AZ31B magnesium alloy. *J. Alloys Compd.* **2015**, *621*, 53–61. [[CrossRef](#)]
152. Majumdar, J.D.; Manna, I. Introduction to Laser Assisted Fabrication of Materials. In *Laser-Assisted Fabrication of Materials*; Springer: Berlin/Heidelberg, Germany, 2013; pp. 1–67. ISBN 9783642283598.
153. Tan, C.; Zhu, H.; Kuang, T.; Shi, J.; Liu, H.; Liu, Z. Laser cladding Al-based amorphous-nanocrystalline composite coatings on AZ80 magnesium alloy under water cooling condition. *J. Alloys Compd.* **2017**, *690*, 108–115. [[CrossRef](#)]
154. Liu, J.; Yu, H.; Chen, C.; Weng, F.; Dai, J. Research and development status of laser cladding on magnesium alloys: A review. *Opt. Lasers Eng.* **2017**, *93*, 195–210. [[CrossRef](#)]
155. Bu, R.; Jin, A.; Sun, Q.; Zan, W.; He, R. Study on laser cladding and properties of AZ63-Er alloy for automobile engine. *J. Mater. Res. Technol.* **2020**, *9*, 5154–5160. [[CrossRef](#)]
156. Siddiqui, A.A.; Dubey, A.K. Recent trends in laser cladding and surface alloying. *Opt. Laser Technol.* **2021**, *134*, 106619. [[CrossRef](#)]
157. Song, G.; St. John, D. Corrosion performance of magnesium alloys MEZ and AZ91. *Int. J. Cast Met. Res.* **2000**, *12*, 327–334. [[CrossRef](#)]
158. Majumdar, J.D.; Maiwald, T.; Galun, R.; Mordike, B.L.; Manna, I. Laser surface alloying of an Mg alloy with Al + Mn to improve corrosion resistance. *Lasers Eng.* **2002**, *12*, 147–169. [[CrossRef](#)]
159. Guo, Y.; Wang, S.; Liu, W.; Xiao, T.; Zhu, G.; Sun, Z. The Effect of Laser Shock Peening on the Corrosion Behavior of Biocompatible Magnesium Alloy ZK60. *Metals* **2019**, *9*, 1237. [[CrossRef](#)]
160. Lim, H.; Kim, P.; Jeong, H.; Jeong, S. Enhancement of abrasion and corrosion resistance of duplex stainless steel by laser shock peening. *J. Mater. Process. Technol.* **2012**, *212*, 1347–1354. [[CrossRef](#)]
161. Shen, X. Laser shock peening in the medical sector: An overview. *Laser User* **2019**, *93*, 20–21.
162. Luan, B.L.; Yang, D.; Liu, X.Y.; Song, G.L. Corrosion protection of magnesium (Mg) alloys using conversion and electrophoretic coatings. *Corros. Magnes. Alloys* **2011**, *2*, 541–564.
163. Han, E.H.; Zhou, W.; Shan, D.; Ke, W. Chemical conversion coating on AZ91D and its corrosion resistance. *Magnes. Technol.* **2004**, *2004*, 121–123.
164. Song, G.-L.; Xu, Z. Surface processing and alloying to improve the corrosion resistance of magnesium (Mg) alloys. In *Corrosion Prevention of Magnesium Alloys*; Elsevier: Amsterdam, The Netherlands, 2013; pp. 110–134.